Chapter 5 Photophysical Radiationless Transitions

5.1 Photophysical Radiationless Transitions as a Form of Electronic Relaxation

In Chapter 4 we were concerned with the portion of the working paradigm of molecular organic photochemistry (Scheme 1.1) that involved radiative processes or absorption and emission (Sch. 4.1). In this Chapter we are concerned with the portion of the working paradigm of molecular organic photochemistry that involves the photophysical radiationless transitions (Sch. 5.1) that are initiated from excited states of organic molecules, in particular those that are initiated from the lowest excited singlet (*R = S_1) state and triplet state (*R = T_1). The importance of the *R(S_1) and *R(T_1) states in organic photochemistry results from the operation of Kasha's rule for Photophysical and photochemical processes in solution and solids: namely that the radiationless deactivations *R(S_n) → *R(S_1) and *R(T_n) → *R(T_1) are much faster than any photochemistry or radiative emission from S_n or T_n. As a result the simplified state energy diagram (Fig. 1.3) is the starting paradigm for the analysis or organic photochemistry in solution. Radiationless processes from S_n or T_n deactivations may be purely vibrational or both electronic and vibrational.

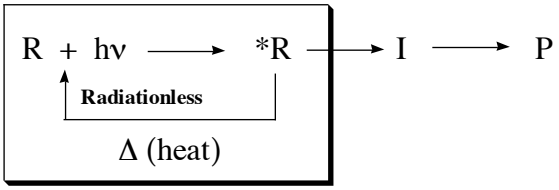

*R(S_n) ⟶ *R(S_1) + Δ (Internal Conversion)

*R(T_n) ⟶ *R(T_1) + Δ (Internal Conversion)

---

*R(S_1) ⟶ R(S_0) + Δ (Internal Conversion)

*R(S_1) ⟶ *R(T_1) + Δ (Internal Conversion)

*R(T_1) ⟶ R(S_0) + Δ (Intersystem Crossing)

Scheme 5.1 Radiationless photophysical transitions of interest to molecular organic photochemistry.

Radiationless transitions between electronic states may be considered as a form of electronic relaxation by which electronic energy is converted into the kinetic energy associated with nuclear motion.[1] In this chapter we shall be concerned with the answers to questions about radiationless transitions such as: What factors determine the rates and efficiencies of internal vibrational and electronic radiationless transitions (which involve no change of electron spin) and intersystem crossings (which involve a change of electron spin)? What are the relationships between the rates and probabilities of radiationless processes and the electronic configurations of the states undergoing the processes? What are the relationships between the rates and probabilities of radiationless processes and quantum mechanical concepts? How can radiationless processes by visualized in terms of molecular mechanisms and representative points on energy surfaces? How are radiationless photophysical processes related to radiationless photochemical processes?

This chapter provides a structural and mechanistic basis for answering these questions, based on fundamental quantum mechanical principles. Photophysical and photochemical radiationless transitions may not always be sharply distinguished. The latter can be treated as being analogous to photophysical processes, except that the conversion of electronic energy into nuclear energy causes such a distortion of the original ground state structure that the molecule does not return to its original nuclear geometry of the ground state spectroscopic minimum, S_0 (a photophysical process) but a new species, I or P is formed (a photochemical process has occurred). The conclusions and generalities made for photophysical radiationless processes in this Chapter will be extended to photochemical radiationless transitions in Chapter 6.

5.2 A Classical Interpretation of Radiationless Electronic Transitions as the Motion of a Representative Point on Electronic Energy Surfaces

Radiationless transitions between two electronic states in quantum mechanics corresponds to a radiationless transformation of two electronic wavefunctions, say, Ψ_1 and Ψ_2. As we have done earlier we shall seek "quantum intuition" to estimate the plausibility of such radiationless electronic transitions by first appealing to a classical paradigm for radiationless transitions to obtain "classical intuition" and then translate the classical interpretation in order to obtain "quantum mechanical intuition".

A classical interpretation[2] of radiationless electronic transitions treats the latter in terms of motion along, or jumps between, energy surfaces by a point which represents the ***instantaneous nuclear configuration*** This point is termed the ***representative point***. (). The representative point will make a radiationless "jump" from one electronic surface to another at certain "critical" nuclear configurations, r_c. These critical geometries will generally correspond to nuclear configurations for which two (or more) energy surfaces come close together in energy or for which there is a minimum on the excited electronic surfaces. The classical intuition concerning radiationless transitions suggests (1) that when two states get close to one another in energy and geometry, the conditions for ***resonance*** are good and a resonance coupling of the two states, followed by a transition between the two states is plausible or (2) that when there is a minimum on an excited surface the representative point persists at that geometry for a period of time and therefore a transition to a lowered energy state is plausible.

According to classical theory of radiationless jumps between surfaces[2] the probability, P, that the representative point will make a jump as r_c is approached is given be the expression Eq. 5.1:

$$P(\text{Probability of surface jump at } r_c) \sim \exp -\Delta E/\nu\, \delta s \qquad (5.1)$$

In Eq. 5.1, ΔE is the energy separation between the surfaces involved in the transition at r_c, ν is related to the velocity (kinetic energy) of the nuclei as they approach r_c, and δs is related to the difference in the values of the slopes of the two surfaces in the region near r_c (we note that dE/dr, the slope of an energy curve, is directly related to the nuclear coulombic ***forces*** (positive charges) acting on the negative electrons and therefore

corresponds to the interactions that will change the motions of the electrons). From Eq. 5.1 we note that since the energy term appears as a negative exponential, ***the probability of a jump will decrease as ΔE increases and will increase as v increases or as δs decreases***. The limiting probability of 1 for a surface jump is expected when the energy difference, ΔE, between the two surfaces approaches 0, when the velocity, v, on a surface is very high and when the difference in slopes, of the surfaces, δs, is small. These features of Eq. 5.1 will provide us with a powerful classical intuition with regard to the probability of radiationless transitions between electronic surfaces, in particularly between an electronically excited surface and a lower energy surface, excited or ground.

The classical interpretation of radiationless transitions first ascribes the simplicity of the motion of a representative point in the regions where the surfaces are well separated. When two energy surfaces are separated by a large energy gap, ΔE, the probability of a transition to the lower surface is very small according to Eq. 5.1 (note the exponential dependence of the rate on -ΔE). Thus, the motion of the representative point continues on the initial surface and continues on the single initial surface until the nuclei attain a critical geometry, r_c, corresponding to a region where ΔE = 0 or close to 0. From Eq. 5.1, we obtain the classical intuition that in regions ΔE = 0, there is the greatest probability ($P \rightarrow 1$, as $\Delta E \rightarrow 0$) of the representative point jumping to a lower surface, so we will seek to answer the question, ***what are the pathways of the representative point which will bring two surfaces close together in energy and how can we deduce these pathways from consideration of molecular electronic structure***.

As we have done previously, we now start with the classical picture of transitions on an energy surface as a basis for developing a pictorial model of the quantum mechanical situation and the behavior of wavefunctions Ψ_1 and Ψ_2 as the representative point moves along a surface corresponding to the energy of one of the wavefunctions. Consider Figure 5.1 which schematically shows the energy of two states Ψ_2 and Ψ_1 as function of a changing nuclear geometry. As the nuclear geometry changes from left to right, the energy of Ψ_1 goes up and the energy of Ψ_2 goes down. We imagine that the representative point starts in the state Ψ_2. Fig. 5.1shows three possible exemplar situations for a representative point whose motion, from left to right, is indicated by the arrows on the surface. Suppose that Ψ_2 initially (geometries to the left of Fig. 5.1)

corresponds to an electronically excited state (*R) and that Ψ_1 initially corresponds to the ground state of R. Then as the representative point moves from left to right, initially it is in an electronically excited state, but after it passes r_c it is in another state. The unspecified x-axis corresponds to a specific change in nuclear configuration of the system. This change is nuclear geometry is loosely termed the "***reaction coordinate***" that is followed by the representative point (even when there is no net reaction, but only a net radiationless processes within the states of a single molecule R.

Figure 5.1a corresponds to a "true" *surface crossing* situation which in Zero Order, the surfaces for the wavefunctions Ψ_1 and Ψ_2 cross and but not interact. When there is a surface crossing the representative point which starts on the surface corresponding to the initial electronically excited state (corresponding to the wavefunction Ψ_2) maintains its electronic characteristics as it crosses the lower energy electronic state Ψ_1, i.e., the states do not mix (interact) in the region near r_c. In the case of a surface crossing the probability, P, of a radiationless transition from the excited surface before r_c to the lower surface is 1.0. what we mean by this is that the wavefunction Ψ_1 which initially was higher in energy than Ψ_2 becomes lower in energy than Ψ_1 at r_c and as a result even though the wavefunction has not changed its essential character, ***it has gone from being an excited state wavefunction to a ground state wave function***. If the geometry of Ψ_1 after passing r_c is similar to the geometry of R, then a radiationless transition to R will have occurred. We shall develop a 3 dimensional description of surface crossings (or weakly avoided crossings) in Chapter 6. In this chapter we shall use the simpler 2 dimensional description to describe photophysical radiationless processes.

r_c = critical nuclear geometry corresponding to a Zero Order surface crossing

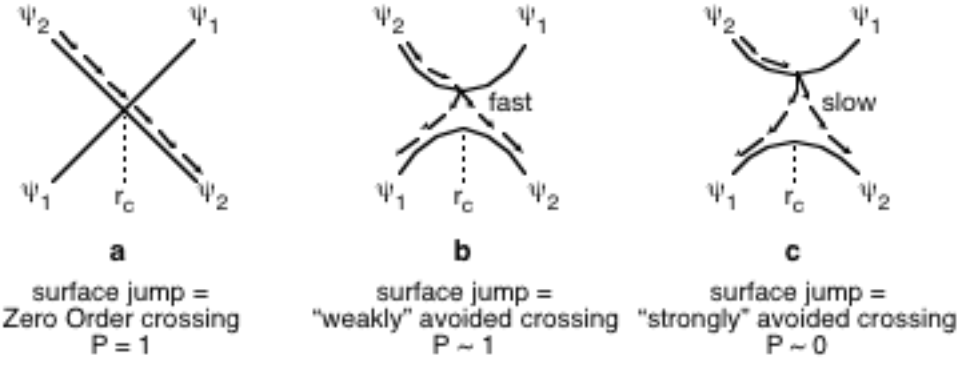

Figure 5.1 ***Representation of the dynamics of a representative point (motion represented by arrows) on an energy surface.***

Figure 5.1b corresponds to a surface crossing at r_c that is a "weakly avoided" crossing, i.e., ΔE is "small" at r_c, and a small mixing of the states occurs at this nuclear geometry. According to the classical expression 5.1, the probability of a surface crossing at r_c is plausible at r_c since ΔE is small, and the representative point has a high probability of jumping from the higher energy surface to the lower energy surface. Again the probability of a radiationless transition is close to 1.0. Depending on the speed at which the representative point approaches r_c it may either continue on it trajectory "to the right of r_c" or leak to a certain extent "to the left of r_c". The differences between the true surface crossing and a weak surface avoiding are subtle, but they both possess the same feature with respect to experimental interpretation: ***radiationless transitions corresponding to situations shown in Fig 5.1a or Fig. 5.1b will be the fastest possible for electronically excited states and in the limit will be rate determined only by the rate of vibrational relaxation.*** Later in this Chapter (Section 5.8) we shall provide experimental examples of the rates of radiationless processes at surface crossings or near surface crossings.

In contrast to Fig. 5.1a and Fig. 5.1b, the surface situation Fig. 5.1c corresponds to a "strongly avoided" crossing at r_c , i.e., ΔE is "large" at r_c. In quantum mechanical terms. this means that the original Zero Order approximation for the wavefunctions near geometries corresponding to r_c is not a good one and that the two surfaces in Fig. 5.1c corresponds to essentially independent and adiabatic wavefunctions. In this case, the jump of the representative point from any where on the excited surface near r_c is slow because ΔE is large throughout the trajectory of the representative point on the excited surface. We therefore expect the representative point to spend a certain amount of time near the excited surface minimum produced by the "avoided" crossing near r_c. A jump from the upper surface to the lower surface may occur from this region of the excited surface, but is expected at a relatively slow rate (compared to the situations in Fig. 5.1a and Fig. 5.1b) because of the large energy gap between the surfaces along the reaction coordinate. Because the representative point has reached a certain equilibrium at r_c, the

jump of the representative point to lower energy may occur in the direction of Ψ_1 or Ψ_2 as indicated by the arrows in Figure 5.1c. The latter possibility indicates the intimate relationship between photophysical and photochemical radiationless transition. Suppose the jump to the right in Figure 5.1c corresponds to a radiationless photochemical reaction, $\Psi_1(*R) \rightarrow \Psi_2(I)$ or $\Psi_1(*R) \rightarrow \Psi_2(P)$ and that the jump to the left in Figure 5.1c corresponds to a radiationless photophysical transition, $\Psi_1(*R) \rightarrow \Psi_2(R)$. In each case the same system near r_c.is making a radiationless transition to a ground state. In one case (jump to the right) we classify the radiationless transition as a photochemical reaction; in the other case (jump to the left) we classify the radiationless transition as a photophysical transition. Let us now consider the wave mechanical interpretation of jumps between surfaces in order to clarify the basis for determining the magnitude of the "electronic coupling" that is required to cause Zero Order crossings to be avoided.

5.3 Wave Mechanical Interpretation of Radiationless Transitions between States

As in classical mechanics, wave mechanics also treats the problem of radiationless transitions in terms of the motion of a representative point on energy surfaces following a reaction coordinate.[3] In order to calculate from wavefunctions the electronic *potential energy* surfaces from wavefunctions, a number of simplifying assumptions are necessary. As discussed in Sections 2.2, solution of the Schroedinger wave equation must be made under the assumption that nuclear and electronic motion are separable and that the electrons instantaneously respond to the changing nuclear motion (Born-Oppenheimer approximation). This approximation allows the solution of the electronic wave equation to be formulated in terms of the motion of *nuclei* only (because for each nuclear geometry it is assumed that there is only one electronic distribution. This process of computing electron distributions is also termed *the adiabatic approximation*, and energy surfaces generated under such assumptions are termed *adiabatic* surfaces. As in the case of classical surfaces, in quantum mechanics the dynamics of nuclear motion on adiabatic surfaces are also treated in terms of the motion of a "representative point" which represents the instantaneous nuclear configuration which determines the electronic distribution. The adiabatic potential energy surfaces are

determined by the solution of the electronic Schroedinger equation for a large number of nuclear geometries (selected as the reaction coordinate) and the lowest energy geometries are determined. The resulting energy surface represents the lowest energy nuclear geometries for a given electronic state, whether it is the ground state or an excited state.

If the changes in the electronic energy of a molecule brought about by nuclear motions are essentially adiabatic (i.e., if the Born-Oppenheimer approximation is a good one), then the behavior of the motions of the electrons may be treated by solution of the wave equation for stationary nuclei. The problem of evaluating electron motion as a function of nuclear motion is the same as that for vibrations between nuclei of a molecule or for the making and breaking of bonds between nuclei in chemical reactions. The differences between the vibrations and chemical reactions are only in the extent of nuclear motion and the occurrence of different equilibria positions for nuclear motions of the reactants and products. If the electron motions are treated as *adiabatic* (i.e., completely and continuously and instantaneously adjusting to changes in nuclear structure), and if the nuclear motions are treated as classical, one can in principle evaluate the electronic potential energy for all nuclear configurations. This is how one generates adiabatic electronic potential-energy surfaces. *For the purposes of radiationless transitoins, the actual motions of the nuclei follow the rules of classical mechanics, and the motions of the nuclei are completely subject to the control of the adiabatic surface.* Thus, the motions of nuclei are wholly determined by the potential-energy surfaces "on which" the *representative point* (or more loosely speaking, the *structure of the molecule*) happens to be. Thus, this justifies the use of classical ideas for radiationless transitions between energy surfaces as a plausible basis for developing an intuitive wave mechanical interpretation of transitions between surfaces.

Figure 5.2 interprets the three exemplar situations of Fig. 5.1 in terms of quantum mechanics and adds one other important example. The four exemplars of Fig. 5.2 will provide a convenient framework for discussing common surface relationships and radiationless transitions between energy surfaces from a wave mechanical point of view: (a) a “perfect” Zero Order crossing; (b) a weakly avoided crossing for which the magnitude of the avoiding is of the same order as vibronic coupling of electron motion; (c) a strongly avoided crossing for which the magnitude of the avoiding is much larger

than vibronic coupling; (d) a "matching" of energy surface which are separated in energy and not related electronically (compare perfect matching to perfect crossing).

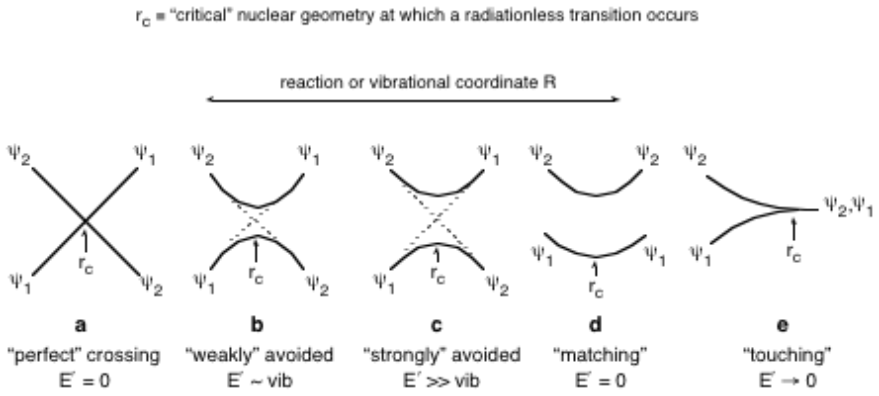

Figure 5.2 ***The archetype adiabatic surface topologies for a two surface system: (a) "perfect" crossing for which Ψ_1 -> Ψ_2 transitions are strictly forbidden; (b) and (c)*** **"weakly" and "strongly" avoided crossings for which Ψ_1 —> Ψ_2 transitions are possible near r_c (see text); (d) "matching" for which Ψ_1 —> Ψ_2 transitions are very improbable (see text).**

Now let's see how quantum mechanics treats the surface situations of Fig. 5.2. In practice approximate electronic wavefunction ψ rather than the true electronic wavefunction Ψ must be employed in making computations. For each case we suppose that the reaction coordinate (change in nuclear configuration) brings the nuclear configuration of a molecule of interest from an initial state (either ψ_1 or ψ_2) into a region corresponding to a Zero Order crossing at geometry r_c. This situation is optimal for mixing of Zero Order states, i.e., near r_c

$$\text{Initial state } \psi_2 \rightarrow \underset{\text{mixing}}{[\psi_2 \pm \psi_1]} \rightarrow \psi_1 \text{ or } \psi_2 \text{ Final state} \qquad (5.2)$$

We say that the Zero Order states ψ_2 and ψ_1 are capable of engaging in electronic resonance near r_c. If resonance should occur, the electron motion is no longer adequately defined in terms of one Zero Order function alone, i.e., the adiabatic (Born-Oppenheimer) approximation is no longer appropriate because the nuclear motion and the motion of the representative point are no longer unambiguously controlled by a single surface ψ_2 or ψ_1, but by a mixed state $[\psi_2 \pm \psi_1]$. What happens when the system which is initially

prepared in state ψ_1 enters the crossing region,[4] i.e., when the representative point of an initial electronic state approaches the "critical" geometry r_c (see Fig. 5.2)?

The energy surface exemplars shown in Figure 5.3 a, b and c are very common in photophysical (this Chapter) and photochemical processes (Chapter 6). If the system corresponds (Figure 5.3a) to Zero Order there is a fast passage through nuclear geometries near r_c and no mixing of ψ_2 and ψ_1, i.e., the motion of the representative point along the reaction coordinate will be completely all on one surface, ψ_2, which corresponds to an excited state surface before r_c and a ground state surface after r_c. A similar situation (Figure 5.3b) will occur if the mixing of ψ_1 and ψ_2 is small near r_c, i.e., a formal "jump" or non-adiabatic transition will occur between the adiabatic surfaces. Notice that in this case the nature of the wavefunction changes on each of the adiabatic surfaces near r_c. The upper surface starts out "pure" ψ_1 until it approaches r_c, where ψ_1 begins to mix weakly with ψ_2. After proceeding beyond the upper surface again becomes "pure" ψ_1! However, since the mixing of the wavefunctions is weak near r_c, the representative point "prefers" to continue to "look like" ψ_1 through out its trajectory and there is a high probability that it will made a jump from the upper adiabatic surface to the lower adiabatic surface.

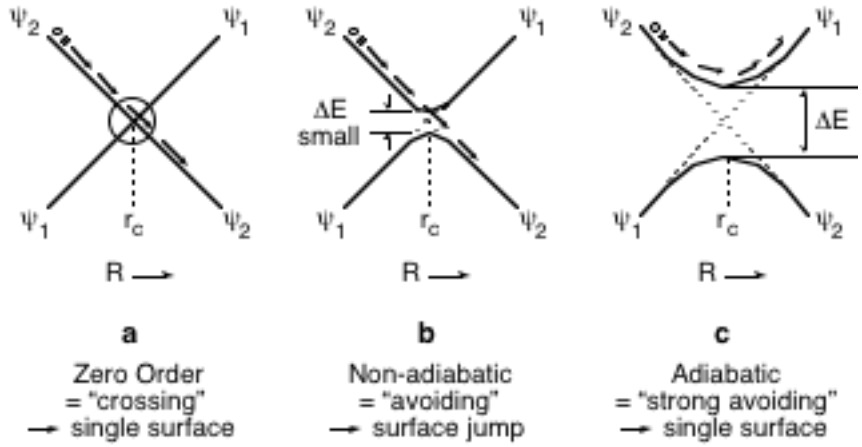

Figure 5.3 ***Schematic representations of the trajectories of a representative point: (a) ψ_2 —> ψ_2 via an adiabatic (no surface jump) pathway along a Zero Order crossing, (b) ψ_2 —> ψ_2 via a nonadiabatic (surface jump) pathway including a weak "avoiding", (c) ψ_2 —> ψ_1 via an adiabatic pathway (no surface jump).***

In the case where there is a large electronic interaction between ψ_1 and ψ_2 near r_c, the two adiabatic surfaces quantum mechanically "avoid" each other and are separated by a large energy gap, ΔE, near r_c. The representative point starting on ψ_2 will easily "switch" over to ψ_1 near r_c, and will "prefer" to remain on the same upper adiabatic surface rather than jumping to the ground state. This means that the representative point has no great difficulty in "looking like" ψ_1 or ψ_2 in the region near r_c. If the representative point gets "stuck" in an excited state minimum for a long enough period of time, an interaction may occur to cause a radiationless transition to the lower surface. This may be viewed as occurring via the dynamic link (dotted lines) provided by the Zero Order crossing. For example, as the molecule is vibrating in the excited state, a small perturbation may couple the excited and ground states and the representative point may be thought to follow the trajectory of the Zero Order surfaces (dotted lines in Fig. 5.3c). Whether the representative point falls to the ground state and proceeds to ψ_1 and ψ_2 will depend on the particulars of the perturbation and the dynamics of the motion of the representative point.

In the region near r_c, if a resonance between ψ_1 and ψ_2 occurs, then there will be an oscillation (resonance) such that the electron motion may be described by either $\psi_1 + \psi_2$ or $\psi_1 - \psi_2$, i.e., the two electronic states are strongly mixed. Although in quantum mechanics such oscillations are "formal", or only imaginary, we can obtain some insight to the time scale of electronic "mixing" by considering the relationship between frequency and energy, i.e., since $\Delta E = h\nu$, then $\nu = \Delta E/h$. since the time, τ, of a vibration is the inverse of the frequency, Eq. 5.3 provides a relationship between the energy gap, ΔE between two electronic states and the time it takes one to "oscillate" its structure into that of the other. We can loosely term the frequency of these imaginary oscillations back and forth as an *electronic tautomerism.*[4b] In the limit of perfect resonance the "lifetime" τ that the molecule spends in a tautomeric form is of the order of

$$\tau \text{ ("lifetime" of an electronic tautomer)} = h/\Delta E \sim 10^{-13}/\Delta E \text{ sec} \qquad (5.3)$$

where ΔE is the resonance energy in kcal/mole. Clearly if a switch from one "electronic" tautomer to another is to occur it must happen within the time $\Delta\tau$ that the molecule is in the region of crossing of surfaces, i.e., $\tau < \Delta\tau$. The stronger the electronic interaction (ΔE), the faster the flip from one electronic state another can occur.

This computation provides us with a benchmark for the time scales of mixing of electronic state as the representative point moves along the reaction coordinate through the critical region near r_c. Strong resonance interactions (e.g., crossings of states of the same electronic and spin symmetries) are of the order of >30 kcal/mole. This corresponds to a lifetime (Eq. 5.3) of an individual electronic tautomer (resonance structure) of $\tau = 10^{-15}$ - 10^{-14} sec via nuclear perturbations occurring at a rate of $1/\tau$.

If the relative velocity of the nuclei moving through the crossing region is $\sim 10^4$ - 10^5 cm/sec = 10^{12}-10^{13} Å/sec (typical values for the vibrations of light atoms) then the time $\Delta\tau$ the nuclei spend in a given region (say, along a line of length of ~3Å) is $\sim 10^{-12}$ - 10^{-13} sec. This rough calculation shows that the lifetime of the tautomer is *shorter* than the time it takes to cross the interaction region. Thus, the tautomerization is complete before the nuclei can move out of the interaction region. In the case of "weak" resonance interaction (<1 kcal/mole), the lifetime of the tautomer is $\sim 10^{-13}$ or longer. Thus, tautomerization may or may not occur in the interaction region, depending on the velocity of the representative point and the precise value of τ.

Frequency of electronic tautomerization $\quad \nu = 1/\tau = \Delta E/h = 10^{13}\ \Delta E$ (in kcal/mole) $\quad$ (5.4)

5.4 Radiationless Transitions and the Breakdown of the Born-Oppenheimer Approximation

We have learned that radiationless transitions between surfaces are difficult at geometries for which the adiabatic electronic surfaces are far apart (more than several vibrational quanta) in energy.[3,5] On the other hand, *radiationless transitions are most probable at geometries, r_c corresponding to crossings of the Zero Order adiabatic*

surfaces. These geometries correspond to "leaks" or funnels in surfaces, and radiationless "jumps" are expected to occur with their highest probability when the representing point corresponds to a geometry "in the region" of a Zero Order adiabatic crossing.[3] These are precisely the regions in which the electronic wavefunction is a rapidly changing (orbital and/or spin) function of nuclear geometry. As the representative point passes through such a region, the nuclear motion has a certain probability of being controlled by *either* electronic surface.

5.5 Crucial Geometries Along the Excited State Reaction Coordinate

Now we return to Figure 5.3, which displays four common surface dispositions along a reaction coordinate. The main idea of a classification of surfaces is to provide some insight into possible radiationless transitions at certain "crucial" molecular geometries which correspond to a region near r_c along the reaction coordinate.

For the "perfect crossing" and “perfect matching” situations (no interaction between wavefunctions at r_c), the electronic interaction energy E' between the initial and final states is precisely zero at r_c and all other geometries. For these situations, the representative point on ψ_2 would have no "knowledge" of the existence of ψ_1 and would pass through the "crossing region" (geometries close to that of r_c) completely unperturbed, i.e., ***the states do not mix at any geometries along the reaction coordinate***. Such a situation is idealized, i.e., rigorously valid only for certain highly symmetric geometries. It is postulated that small distortions from the idealized geometries do not significantly modify the conclusions based on the Zero Order crossing. As a rule, if the coupling between ψ_1 and ψ_2 in the region near r_c is much less than the energy of vibrational couplings (<100 cm^{-1}), we may consider $E' \sim 0$. However, a close approximation to a "perfect crossing" is one for which the two states differ in spin multiplicity and for which spin-orbit coupling is weak, i.e., most singlet-triplet surface crossings involving aromatic hydrocarbons.

For the "weakly avoiding" situation, the electronic coupling (in First Order) between ψ_1 and ψ_2 at r_c may be of the order of vibrational energies but not much greater. In Figures 5.2 and 5.3, dotted lines are drawn to serve as a reminder of the Zero Order crossing. For the "strongly avoiding" situation, the electronic coupling (in First Order) between ψ_1 and ψ_2 at r_c is much larger than vibrational energies, thus the ground state and excited state surfaces are far apart at all geometries along the reaction coordinate, inhibiting radiationless transitions to the ground state. In the "matching" situation as in the Zero Order crossing situation, ψ_1 and ψ_2 does not possess any electron coupling even in First Order. Thus, one must proceed to a Second or higher order perturbation if ψ_1 and ψ_2 are to be coupled. We note the shape for the ground and the excited surface for the strongly avoided crossing shows a minimum in the excited state and a maximum in the ground state. The example in Fig. 5.2d is shown with a minimum at r_c in the excited states in order to make this a critical point on the reaction coordinate. However, a large number of relative shapes of the ground at r_c are possible, since there is no interactions between the states and their relative.

Although many Zero Order crossings are "avoided" to a greater or lesser extent (see Fig. 5.1), for real crossings or weakly avoided crossings the molecule either stay on the initial surface or readily jumps from one adiabatic (First Order) surface to another, i.e., the representative point follows the Zero Order surface (for which electronic configuration or multiplicity is preserved). Such regions of surface crossings or weak surface avoiding are referred to collectively as "holes" or "funnels" in an upper surface and plan an essential role in photophysics and photochemistry.[3b] As the crossing becomes more strongly avoided (Fig. 5.3c), the probability of jumps between adiabatic surfaces in the region of the geometry corresponding to Zero Order surface crossing decreases. In the limit a "funnel" becomes a true excited state "minimum" which is detectable by conventional flash spectroscopic and/or chemical trapping methods.

"Leaks" or "jumps" from one surface to another occur most readily when they can occur with very little nuclear geometry change and with little change in nuclear momentum. The greater the change in nuclear geometry or in nuclear momentum which results from a surface jump, the more strongly the leak or jump is resisted, i.e., the slower the rate of the radiationless transition from one surface to another.

An essential difference between the "strongly" avoiding and "matching" topologies is the occurrence of a "Zero Order" linkage (dotted lines) between the upper and lower surfaces in the former, which does not occur in the latter. The importance of this distinction is that for an avoided crossing the representative point may jump from ψ_2 to ψ_1 in the region near r_c, because the dotted line (Zero Order connectivity) provides a "dynamic" link between the upper and lower surfaces. When surfaces are "matched" near r_c, there is no dynamic link coupling them at the purely electronic level. The "strongly avoiding" topology occurs typically near geometries which correspond to transition states for "allowed" pericyclic reactions.

A final surface situation to be discussed in Chapter 6 is termed "touching". In this case, the two electronic surfaces approach each other asymptotically, and at or near r_c they become very close in energy, i.e., they essentially "touch" each other. Such a surface topology near r_c would be typical for certain states during the breaking of a σ bond or a π bond (see Section 6.x, especially Fig. 6.8 and 6.9). A surface touching, like a surface crossing or weakly avoided crossing, serves as a “funnel” for radiationless transitions from an upper energy surface to lower energy surface. However, in the case of surface touchings, progress beyond r_c correspond to chemical reactions.

5.6 Conical Intersections Near Zero Order Crossings

The “non-avoiding” crossing or touching of energy surfaces, while a rare situation for diatomic molecules, turn out to be quite a common situation for organic molecules. The energy surfaces shown in the figures in this chapter are simplified and two dimensional curves, whereas more realistic energy surfaces are multidimensional. If one considered even a three dimensional extension of the energy surface concept, the immediate vicinity of the crossing point in a Zero Order representation becomes a “double cone”, one portion of which corresponds to the upper surface and the other portion of which corresponds to the lower surface. At the touching point of the two cones the wavefunctions for the two surfaces are degenerate. This touching point is termed a “conical intersection” and has recently been found, through computational analysis, to be an important concept in the examination of photochemical processes. Conical

intersections serve as efficient funnels for the representative point to move from an upper surface t a lower surface. In favorable cases, motion through a conical intersection can occur at effectively the rate of zero point vibrational motion. We shall postpone a detailed discussion of conical intersections will be discussed in detail in Chapter 6. However, as noted earlier, very fast ***electronic*** radiationless transitions, i.e., those occurring at rates of vibrational transitions, are often assumed to occur through conical intersections in 3 dimensions (or as described in this Chapter in 2 dimensions as the result of a true or near surface crossing).

5.7 Formulation of a Parameterized Model of Radiationless Transitions

Although complicated in detail, fortunately only a few parameters are necessary for a qualitative evaluation of the probabilities (or relative probabilities) of radiationless transitions. As was done for radiative transitions in Section 4.26 we may consider the *experimental* probability of a radiationless transition (usually expressed in terms of an observed rate constant, k_{ob}) as the product of the rate constant for a hypothetical "fully allowed" (k_o) process; and prohibition factors (f) due to electronic, vibrational or spin factors which contrive to reduce k_o to the observed k_{ob}. Recall the concept of oscillator strength and the various selection rules which lead to a decrease in observed oscillator strengths from an ideal, maximal value of 1.0. In the same spirit we can suppose that k_{ob} may be parameterized[7] as show in Eq. 5.5:

Observed rate: $k_{ob} = k_o \times f_e \times f_v \times f_s$ maximal rate time prohibition factors (5.5)

In Eq. 5.5, f_e, f_v, and f_s represent the "prohibition factors" due to the electronic, nuclear, and spin configurational changes which occur during the radiationless transitions. The magnitude of term f_e is related to the magnitude of the matrix element for the *pure electronic part* of the radiationless transition. The magnitude of f_e may be qualitatively evaluated by inspection of the positive overlap of the *orbitals which change* during the radiationless transition. The magnitude of f_v is related to the magnitude of the overlap of

the nuclear wave functions for the initial and final states, i.e., the *Franck-Condon factor* or the prohibition to the probability of transition due to change in vibrational nuclear configuration or motion. Finally, f_s is related to the spin multiplicity in the initial and final states. For organic molecules, the magnitude of f_s will depend on the spin-orbit coupling interactions which occur during an intersystem crossing.

Each one of the factors, f, represents some sort of structural rearrangement, such as an electronic rearrangement (f_e), a vibrational change (f_v), or a spin rearrangement (f_s), which may be rate limiting. In addition, excess electronic energy released by the radiationless transition must be "accepted" somehow, in order to obey the law of energy conservation; however, this energy release is rarely rate-determining since energy can be taken up by intramolecular and intermolecular vibrational energy transfer. The "acceptors" of the excess electronic energy may be either the vibrations of the molecule undergoing the transition or the vibrational, rotational and translation motions of solvent molecules. Thus, intramolecular vibrations and intermolecular collisions typically serve as a "heat bath" that rapidly soaks up the excess electronic energy originally localized in the molecule undergoing the radiationless transition. Let us now show how the transfer of energy (electronic and vibrational) is involved in radiationless transitions of the type given in Sch. 5.1.

5.8 Visualization of Radiationless Transitions Promoted by Vibrational Motion; Vibronic Mixing

In the Zero Approximation we assume that for a given, fixed nuclear geometry the electronic states may be classified in terms of a single electronic orbital configuration and a single spin type (multiplicity). We consider these Zero Order states as "electronically and spin pure," e.g., "pure" n,π* or π,π* states and "pure" singlet or triplet states. In the First Approximation we consider various mechanisms for "mixing" of the states. In First Order, n,π* and π,π* states are mixed to a certain extent by electron-electron interactions and vibrations of a molecule and, as are singlet and triplet states. This mixing “relaxes” selection rules for transitions which are strictly forbidden in Zero Order. In addition to vibronic interactions, spin-orbit interactions all serve to "mix" the Zero Order states.[8]

Let's use a n,π* → π,π* as an exemplar of a vibrationally induced radiationless transition. In terms of orbitals, a n,π* → π,π* radiationless transition corresponds to a one-electron jump of a π electron into an n orbital (we assume that π* electron does not change during the transition), i.e., we may consider the main electronic change in the transition to correspond to a π → n orbital jump (Fig. 5.4). For the process to be isoenergetic, vibrational motion must cause a "switching" of the energetic ordering of the n and π levels. It is not absolutely necessary that the π,π* be lower in energy than the n,π* state, but only that a crossing point can be accessible during the lifetime of the excited state and that the system then deactivates along the π,π* surface. In some cases thermal energy (provided by collisions with molecules in the environment) must be provided to the system in order for the crossing point to be reached, i.e., the radiationless process will require an activation energy. The reverse situation of a π,π* → n,π* transition can easily be imagined based on the same simple orbital considerations. In this case the system starts off in a π,π* configuration and a n → π orbital transition occurs.

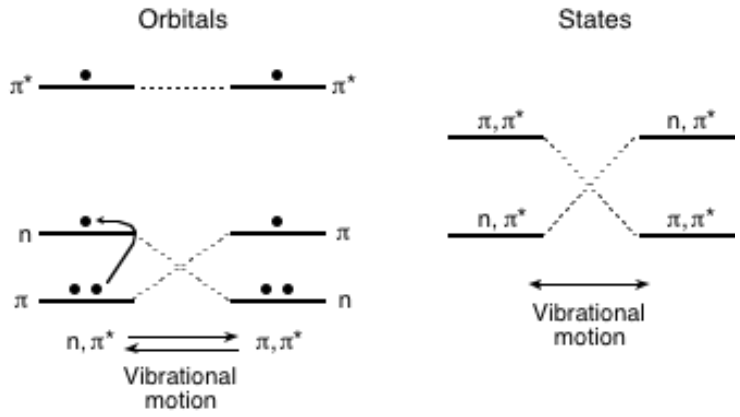

Figure 5.4 ***Orbital and state descriptions of n,π* <— π,π* state switching as a result of vibrational motion.***

From the standpoint of wave mechanics,[9] the largest matrix elements for vibronic interactions are those which vibrations generate oscillating electric dipoles in the same region of space as the transition dipoles for the states undergoing electronic transition. That this should be the case is plausible based on the "quantum intuition" available from discussions of the interactions of oscillating dipoles that modeled the interaction of light and electrons. The "best" vibrations for causing mixture of the n,π* and π,π* states are

those nuclear motions which cause displacement of atoms possessing substantial n and π density. In the case of a ketone, the O atom of the carbonyl group possesses characteristics for mixing n,π* and π,π* states.

We can also deduce from this qualitative analysis that not all vibrations are effective in mixing n,π* and π,π* states. For example, for a ketone in a planar geometry, any vibrations which do not disrupt planarity are not effective in generating electric dipoles near the oxygen atom because the n and π orbitals are orthogonal (possess an electronic overlap integral $\langle n|\pi\rangle = 0$) as long as the system is planar. Non-planar vibrations, on the other hand, cause the p orbitals on oxygen to rehybridize and to pick up s-character (Fig. 5.5). As a result, $\langle n|\pi\rangle \neq$ zero for non-planar geometries. However, the mixing of surfaces due to non-planar vibrations will be weak.

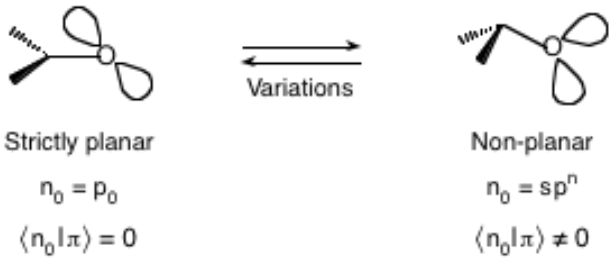

Figure 5.5 ***Schematic of the "mixing" of s character into a p-orbital as the result of nonplanar vibrations.***

Let us consider how "mixing" of states is viewed in terms of energy surfaces (Fig. 5.6). Suppose a Zero Order crossing of an n,π* and a π,π* state of a ketone exists. The occurrences of a surface crossing for a planar vibration and of a surface avoiding for a non-planar vibration are shown in Figure 5.6. It is important to notice that the states are significantly mixed for those geometries only near the crossing point, r_c, where the energies of the two Zero order states are nearly equal. Thus, for geometries near the energy minima on the lower surface in Fig. 5.6, the Zero Order approximation of a "pure" n,π* and "pure" π,π* state is still quite valid.

As a result of a certain nuclear motion (vibrations) the nuclear structure may change from a strictly planar shape (for which the assumption of purity of n,π* and π,π* states is a good approximation) to a non-planar shape (for which the n,π* and π,π* states are

allowed to mix). As a result of this vibronic interaction, the Zero Order surface crossing is removed and replaced by a First Order surface avoided crossing. The magnitude of the avoiding is given by a matrix element of the type:[9]

$$\langle n,\pi^*|H_{vib}|\pi,\pi^*\rangle \qquad (5.6)$$

where H_{vib} is an operator representing the vibrational motion (e.g., C-C-O bending vibration) which causes the mixing of the states. The magnitude of this matrix element may be estimated from the overlap integral $\langle n,\pi^*|\pi,\pi^*\rangle$. Since the overlap of the π^* orbital with itself is unity, then $\langle n,\pi^*|\pi,\pi^*\rangle \sim \langle n|\pi\rangle$, i.e., it is only the overlap of the n and π^* orbitals that determine the effective overlap in eq. 5.5. Although $\langle n|\pi^*\rangle = 0$ for planar vibrations (Figure 5.5, left) $\langle n|\pi\rangle \neq 0$ for non-planar vibrations, which introduce s-character into the π orbital and n orbital.

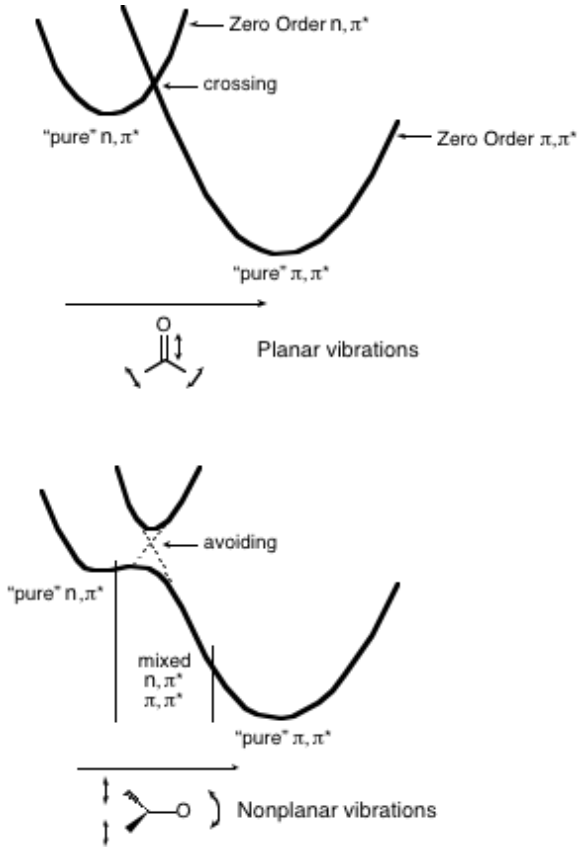

Figure 5.6 ***The effect of planar (top) and nonplanar (bottom) vibrations on a Zero Order crossing of n,π* and π,π* surfaces.***

It is useful and important to have benchmarks for the frequency of vibrational motion of pairs of atoms that commonly occur in organic molecules. As noted in Chapters 2 and 3, vibrational motion between two atoms, X-Y, may be represented as the periodic motion of a harmonic oscillator. The oscillation *frequency* of a harmonic oscillator is related to the restoring force (-kr) and the masses of the particles involved in the oscillation by the expression

$$\nu(\text{frequency of vibration}) = 1/2\pi(k/\mu)^{1/2} \qquad (5.7)$$

where k is the *force constant* (a measure of the "stiffness" of the restoring force, or for a molecule, of the bond strength), and μ is the reduced mass of the atoms involved in the vibration. When the mass of X is much larger than the mass of Y, μ is approximately equal to the mass of Y, i.e., $\mu \sim$ mass of the lighter nucleus.

Table 5.1 lists some frequencies of vibrations for pairs of atoms involved in vibrations in organic molecules for which strongly bonded pairs of atoms may often be treated as an independently vibrating pair. From Eq. 5.7 we expect and find that ν will *increase* with increasing bond strength at constant μ, e.g., ν(C-C) > ν(C-C). We also expect for comparable bond strength that ν will *decrease* with increasing μ, e.g., ν(C-H) > ν(C-D) and ν(C-C) > ν(C-Cl).

5.9 Visualization of Radiationless Transitions Promoted by Spin-Orbit Coupling

From the vector model for electronic spin (Sections 2.7 and 3.6) it was deduced that two possible mechanisms exist for intersystem crossing, a spin "flip" and a spin "rephasing." For organic molecules, spin-orbit interactions usually provide the major mechanism for intersystem crossing, whereas spin-spin interactions provide an alternate mechanism for radical pairs and diradicals.[10]

Consider Fig. 5.7 for a general, schematic interpretation of intersystem crossing in terms of energy surfaces.[10] In the Zero Order approximation (Figure 5.7, top) we assume we do not have a mechanism for intersystem crossing, resulting from our artificial separation of electronic and spin motions. In this approximation if a molecule is in an

initial singlet state it will forever stay in the singlet state, or if it is in an initial triplet state it will remain forever in the triplet state, even if a reaction coordinate exists such that a crossing of the single and triplet state occurs.

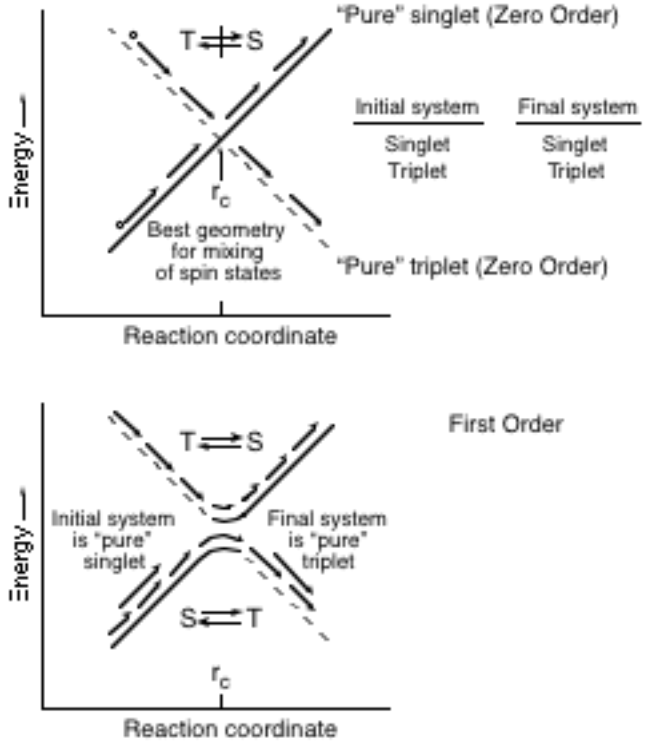

Figure 5.7 ***Intersystem crossing is strictly forbidden in the Zero Order approximation (top figure) but becomes partially allowed when a spin mixing mechanism is available (lower figure).***

When we introduce spin-orbit coupling, it becomes possible that as a representative point moves along an initially "pure" singlet or triplet surface, intersystem crossing may occur near the nuclear geometry corresponding to r_c, *if certain conditions are met*. These conditions are that the interaction that mixes the spin states must be "turned on" and must be effective when the representation point is near r_c. Thus, there is a requirement not only that a force capable of changing the spin multiplicity must exist but also that it must operate effectively during the time period when the representative point is in the region near r_c (i.e., the molecule has a nuclear geometry corresponding to r_c and an energy close to that of the Zero Order crossing point).

Table 5.1 Some Common Bond Types and Associated Stretching Frequencies and Bond Strengths

Bond Type	Vibrational Type	Oscillation period	Bond Strength (kcal/mole)
C=C	stretch 2200 cm^{-1}	= 5.6 x 10^{13} sec^{-1}	100
C=O	stretch 1700 cm^{-1}	= 5.1 x 10^{13} sec^{-1}	180
C=C	stretch 1600 cm^{-1}	= 4.2 x 10^{13} sec^{-1}	165
N=N	stretch 1500 cm^{-1}	= 4.0 x 10^{13} sec^{-1}	110
C-H	bend 1000 cm^{-1}	= 3 x 10^{13} sec^{-1}	100
C-C	stretch 1000 cm^{-1}	= 3 x 10^{13} sec^{-1}	85
C-C	bend 500 cm^{-1}	= 1.5 x 10^{12} sec^{-1}	85
C-H	stretch 3000 cm^{-1}	= 9 x 10^{13} sec^{-1}	100
C-D	stretch 2100 cm^{-1}	= 6 x 10^{13} sec^{-1}	100

5.10 Selection Rules for Intersystem Crossing

In Section 3.20, we learned that spin-orbit interactions for organic molecules which do not possess heavy atoms are effective in promoting intersystem crossing near r_c if: (a) the orbital transition involved possesses the character of a $p_x \rightarrow p_y$ orbital jump to generate orbital angular momentum, and (b) the orbital transition is localized on a single atom.

Let us consider an unsaturated system containing a heteroatom but no heavy atoms. From the standpoint of spin-orbit coupling, such a system introduces a crucial difference relative to an unsaturated aromatic hydrocarbon, namely the occurrence of n,π* configurations. Let us take a carbonyl group as an exemplar for our qualitative analysis of spin-orbit coupling in such containing a heteroatom. The singlet state of a carbonyl group may be derived from an n,π* or a π,π* configuration. Consider the four

possible intersystem crossings from S_1 of a carbonyl group for the different starting and final electronic configurations:

1. $^1n,\pi^* \rightarrow {}^3\pi,\pi^*$ (5.8)

Figure 5.8

2. $^1n,\pi^* \rightarrow {}^3n,\pi^*$ (5.9)

3. $^1\pi,\pi^* \rightarrow {}^3n,\pi^*$ (5.10)

Figure 5.9

4. $^1\pi,\pi^* \rightarrow {}^3\pi,\pi^*$ (5.11)

If we assume that the rate of intersystem crossing is directly related to the magnitude of spin-orbit coupling, then we can estimate the magnitude by inspection of the several configurations of the initial state to determine if there is finite First-Order interaction with any of the configurations of the final state, i.e., if a $p_x \rightarrow p_y$ orbital jump localized on a single atom occurs.[10]

First we consider a $^1n,\pi^* \rightarrow {}^3n,\pi^*$ intersystem crossing (eq. 5.9). Two major atomic orbital representations of the $^1n,\pi^*$ state are shown in Figure 5.8a. Intersystem crossing must involve either an n or a π^* electron spin flip. In neither orbital representation is a First-Order spin-orbit coupling possible because neither the $n(\uparrow) \rightarrow n(\downarrow)$ nor the $\pi^*(\downarrow) \rightarrow \pi^*(\uparrow)$ electronic transitions generate orbital angular momentum along the bond axis; i.e., no $p_x \rightarrow p_y$ single atomic orbital jump is involved. Thus, *there is no First-Order spin-orbit coupling for the $^1n,\pi^* \rightarrow {}^3n,\pi^*$ transition.*

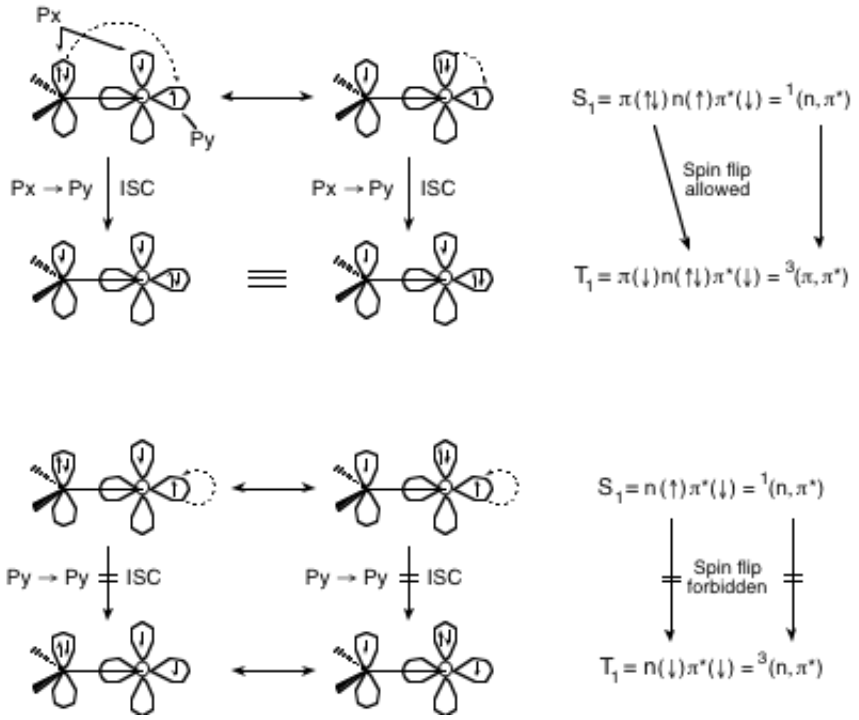

Figure 5.8 ***Qualitative orbital description of the basis for the allowed $^1(n,\pi^*) \rightarrow {}^3(\pi,\pi^*)$ and the forbidden $^1(n,\pi^*) \rightarrow {}^3(n,\pi^*)$ intersystem crossing.***

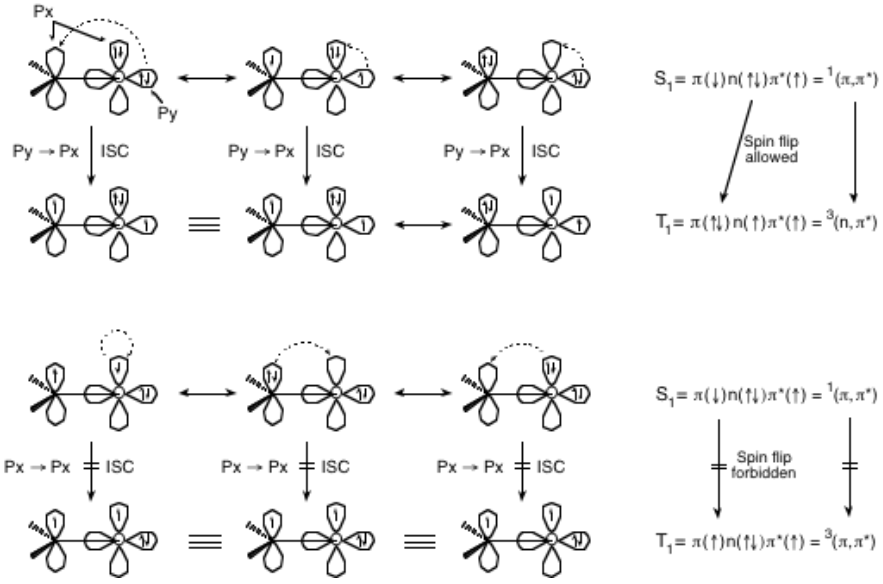

Figure 5.9 ***Qualitative orbital description of the allowed $^1(\pi,\pi^*) \rightarrow {}^3(n,\pi^*)$ and the forbidden $^1(\pi,\pi^*) \rightarrow {}^3(\pi,\pi^*)$ intersystem crossings.***

In contrast, the $^1n,\pi^* \rightarrow {}^3\pi,\pi^*$ transition has a First-Order spin-orbit coupling in one of its major atomic orbital configurations (Fig. 5.8b). As a result, intersystem crossing can be triggered via a one-center $p_x \rightarrow p_y$ interaction. In addition, the highly

electrophlic, half-filled n orbital provides a substantial "driving force" for the electronic transition by attracting one of the electrons from the π orbital.[10]

Starting from a $^1\pi,\pi^*$ state we must consider three atomic orbital configurations (Fig. 5.9). By inspection, two of the atomic orbital configurations have a First Order coupling with a configuration of the $^3n,\pi^*$ state. Thus a $^1\pi,\pi^* \rightarrow {}^3n,\pi^*$ transition is "allowed" to occur by spin-orbit coupling. By inspection of the $^1\pi,\pi^* \rightarrow {}^3\pi,\pi^*$ transition, there is no First Order spin-orbit coupling between any of the singlet configurations and the triplet configuration (Fig. 5.9).

As a result of our analysis we deduce the following selection rules (commonly termed Ed-Sayed's rules)[11] for intersystem crossing of carbonyl groups:

$$n,\pi^* \rightarrow n,\pi^* \quad \text{Forbidden} \tag{5.12}$$

$S_1 \rightarrow T$ transitions

$$n,\pi^* \rightarrow \pi,\pi^* \quad \text{Allowed} \tag{5.13}$$

$$\pi,\pi^* \rightarrow \pi,\pi^* \quad \text{Forbidden} \tag{5.14}$$

The rules derived from this exemplar are general for n,π^* and π,π^* states and are not restricted to carbonyl compounds.

Although more quantitative data is listed in Table 5.4, here we will give examples of an alkyl ketone,[12] benzophenone,[13] and pyrenaldehyde[14] for which the values of k_{ST} are $\sim 10^8$ sec^{-1}, $\sim 10^{11}$ sec^{-1}, and $\sim 10^7$ sec^{-1} respectively. Figure 5.10 summarizes the transitions involved for the cases given by eq. 5.12, 5.13 and 5.14.

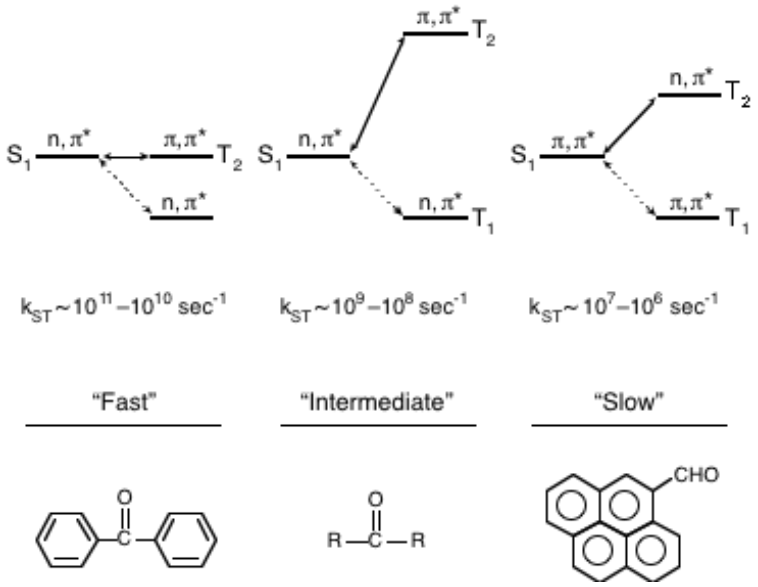

Figure 5.10 ***Examples of different rates of intersystem crossing for $S_1(n,\pi^*) \rightarrow T(\pi,\pi^*)$, $S_1(n,\pi^*) \rightarrow T(n,\pi^*)$ and $S_1(\pi,\pi^*) \rightarrow T(\pi,\pi^*)$, of carbonyl compounds.***

Extending the logic for spin-orbit coupling in $S_0 \rightarrow T_1$, transitions, we deduce that a $p_x \rightarrow p_y$ transition on a singe atom is also optimal for a $T_1 \rightarrow S_0$ intersystem crossing transition, so that

$T_1 \rightarrow S_0$ transitions	$n,\pi^* \rightarrow n^2$	Allowed	(5.15)
	$\pi,\pi^* \rightarrow \pi^2$	Forbidden	(5.16)

The $T_1 \rightarrow S_0$ transitions of benzophenone and acetone (k_{TS} ~ 10-100 sec^{-1}) are much faster than that for pyrenaldehyde ($k_{TS} < 1$ sec^{-1}), which is in agreement with the above selection rules. It should be noted that the actual magnitude of spin-orbit coupling for the excited states of organic molecules is on the order of 0.3-0.001 kcal/mole, i.e., spin-orbit coupling is a very weak perturbation.[10]

For example of the effect of vibrations on spin orbit coupling,[15] consider a surface crossing between a π,π^* singlet and π,π^* triplet state of ethylene or of benzene. The effect of vibrations on spin orbit coupling is a *second order* electronic coupling effect for which a weak interaction (spin orbit coupling) is induced by a second weak

coupling (vibronic coupling). As usual, we look to orbital interactions to introduce the required $\sigma \rightarrow \pi^*$ single atomic orbital jump. In this case since there are no n orbitals to take part in the process we need to invoke σ and σ^* orbitals for interactions with the π,π^* states. This means that vibrations need to mix $\sigma \rightarrow \pi^*$ and $\pi \rightarrow \sigma^*$ transitions, which possess the character of $p_x \rightarrow p_y$ transitions. Since the $\sigma \rightarrow \pi^*$ and $\pi \rightarrow \sigma^*$ transitions are not one center in nature and because the energy gap between the orbitals involved in the transitions are high in energy, the spin orbit coupling mixed in by vibrations is typically very weak.

In-plane vibrations generally do not cause mixing of singlet and triplet states of planar hydrocarbons, but out-of-plane vibrations are capable of (weakly) mixing singlet and triplet states.[16] Figure 5.11 shows the surface situation for in-plane and out of plane vibrations. In executing planar vibrations the molecule may pass through a surface crossing geometry, but will not be able to "turn on" a spin-orbit interactions because the planar vibration is an ineffective promoter for coupling spin and orbital motion. If the molecule is brought into a crossing geometry by an out-of-plane vibration, a finite but very weak spin-orbit interaction occurs, the surfaces avoid, and a $^1\pi,\pi^* \rightarrow {}^3\pi,\pi^*$ conversion is possible ($k_{ST} < 10^7$ sec^{-1}). In effect, the "door is open" at a crossing geometry only if the molecule is conducted to the crossing region by an appropriate vibration or nuclear motion.

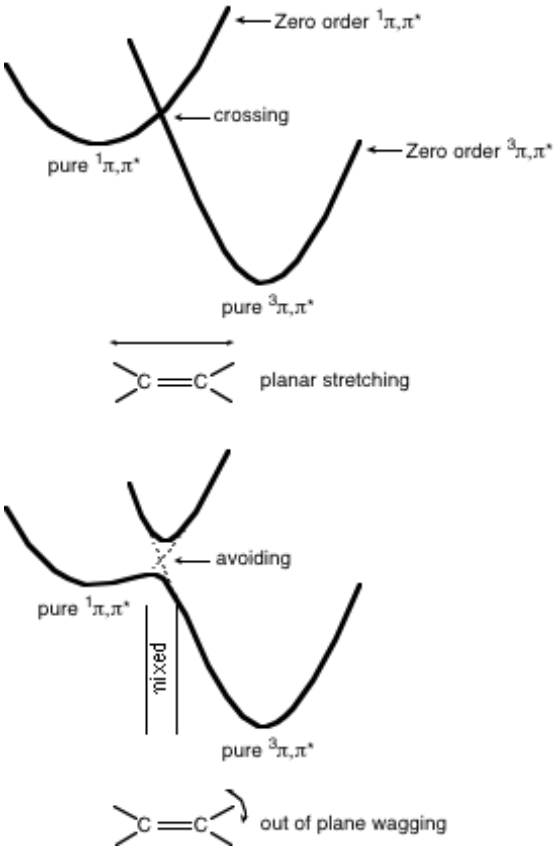

Figure 5.11 ***Vibronic interactions. Top: planar vibrations do not mix states, so that a Zero Order crossing persists in First Order. Bottom: out-of-plane vibrations cause an avoiding.***

5.11 The Relationship of Rates and Efficiencies of Radiationless Transitions to Molecular Structure

The organic photochemist needs a theory that reveals the relationship of the probability of radiationless transitions of electronically excited states to molecular structure. From the discussions of Sections 5.2 and 5.3, it is clear that an important feature of such a theory is the idea of "critical geometries," r_c, from which radiationless transitions are particularly favored. Thus, a theory relating radiationless processes to molecular structure must be able to relate critical geometries to molecular structure.[3] Surface crossings, surface touchings (Chapter 6), and shallow and deep excited state minima all correspond to such critical geometries (Fig. 5.2 and Fig. 5.3). In Chapter 6 we shall consider how one may use correlation diagrams to relate the occurrence of Zero

Order surface-crossings to molecular structure. In this section we consider how "surface touchings" can be related to molecular structure. In Section 5.8 shall see how radiationless transitions from excited state minima that correspond to "surface matchings" may be related to molecular structure.

5.12 The "Loose Bolt" and "Free Rotor" Effects: Promoter and Acceptor Vibrations

It is possible for certain vibrations to act as promoters of radiationless transitions if specific vibrations "carry" the representative point to the region near r_c. However, since energy must be conserved in detail after a radiationless transition, some vibrations (or collisions with molecules in the environment) must act as acceptors of the energy difference between the electronic states involved in the transition. *If a vibration can act as both a promoter and an acceptor it should be particularly effective in triggering radiationless transitions*.[17]

Two exemplar vibrations of organic molecules are the stretching of a single C-C σ bond and the twisting of a C=C π bond. Consider two examples of surface "touchings" induced (1) by stretching a σ bond and (2) by twisting a π bond (Fig. 5.12). A stretching or twisting vibration may escort the representative point on and excited surface (ψ^*) to a region on the surface near r_c. If this same vibration also causes vibronic mixing of ψ^* and ψ^0 a radiationless transition to ψ^0 near r_c then become plausible. In some cases the same vibration serves as a means of accepting excess energy that is involved in the transition between ψ^* and ψ^0. The stretching vibration is analogous to a "loose bolt" in some moving part of a machine. The "loose bolt" tends to be set in motion by other moving parts of the machine [17a] and thereby "takes up" kinetic energy produced by other moving parts of the machine. In the case of the molecule the excess energy may lead to complete dissociation of the bond, i.e., the promoting vibration turns into an irreversible separation of the atoms involved in the vibration.

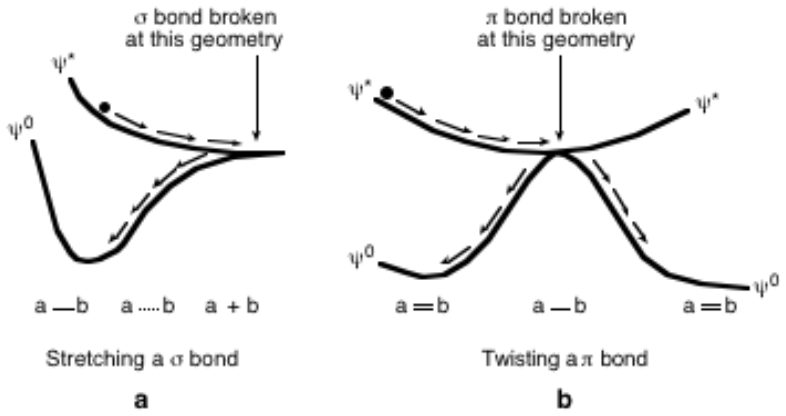

Figure 5.12 ***Schematic representation of (a) the stretching of a σ bond and (b) the bending of a π bond.***

In the case of the twisting motion of a double bond (Fig. 5.12b) in stead of a "loose bolt" the situation is more analogous to a "free rotor" which accepts the excess energy by a rotation seems more apt. In this situation the twisting motion leads to a cis-trans isomerization in the case of twisting about C=C π bonds.

Examples of the free rotor and loose bolt effects on radiationless transitions such as *internal conversions* are available from fluorescence analysis of conjugated aromatic compounds. For example, at 25°C trans-stilbene (**1**) is weakly fluorescent ($\Phi_F = 0.05$) and cis-stilbene (**2**) is non-fluorescent ($\Phi_F \sim 0.00$).[18] On the other hand, the structurally constrained derivatives **3** and **4** are strongly fluorescent ($\Phi_F \sim 1.0$).[19]

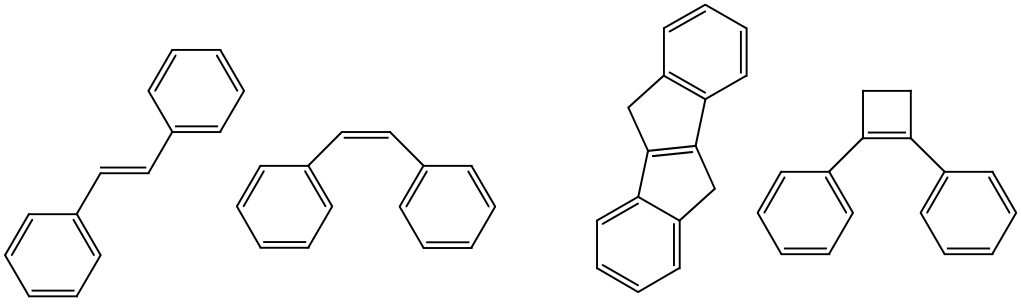

1, $\Phi_F = 0.05$ **2**, $\Phi_F = 0.00$ **3**, $\Phi_F = 1.0$ **4**, $\Phi_F = 1.0$

Steric interactions between the phenyl groups of cis-stilbene provide the molecule with an inherent torque and tendency to twist about the central C=C π bond, introducing a free rotor along the π,π* surface. In S_1 the state energy is rapidly lowered by twisting (See Fig. 5.12b. For a more rigorous discussion, see Section 5.7) The twisting motion brings S_1 to a geometry, r_c, which is favorable for radiationless conversion to S_0. Although **1** can also twist about the C=C bond in S_1, it lacks a torque due to steric interactions and as a result the twisting motion slower for **1** than it is for **2**. Fluorescence can now compete with internal conversion and intersystem crossing.

For compounds **3** and **4** the twisting motion about the C=C bond is severely hindered by structural constraints. As a result, these molecules are relatively rigid and are unable to adopt nuclear geometries that differ substantially from the initial geometry of S_0. The representative point on the S_1 surface cannot move to regions near r_c that correspond to nuclear geometries favorable for radiationless conversions. As a result, fluorescence dominates ($\Phi_F \sim 1.0$). In addition to structural constraints, low temperature and a rigid intermolecular environment can inhibit twisting motions that promote radiationless conversions. If small energy barriers (~3-5 kcal/mole) separate the representative point from the lower energy twisted geometries, at low temperatures (~ 77K) these barriers may not be surmounted during the excited state lifetime and efficient emission results. A rigid environment may be viewed as perturbing the potential energy surface corresponding to rotation by introducing an energy barrier to twisting.[20] These environment (e.g., solvent) imposed barriers are due to the requirement that molecules in the neighborhood of the twisting C=C bond must be displaced if the twisting is to be substantial, a difficult process in a rigid environment.

The free rotor effect may also operate to facilitate radiationless transitions of singlets (internal conversion to S_0 and intersystem crossing to T_1) or triplets (intersystem crossing $T_1 \rightarrow S_0$). As an illustration,[21] the triplet state of 1-phenylcycloheptene (**5**) undergoes a very rapid intersystem crossing at room temperature relative to the more rigid 1-phenylcyclobutene (**6**). This result may be interpreted to be due to a surface

touching (Fig. 5.12b; see Section 5.7 for discussion) which results from twisting about the C=C bond. Since **5** is much more flexible than **6** with respect to this motion, in T_1 it may move toward the twisted geometry at a faster rate:

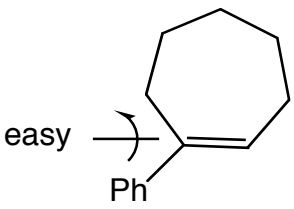

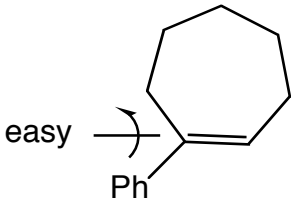

5, $k_{TS} = 4 \times 10^9$ sec^{-1} **6,** $k_{TS} = 6 \times 10^7$ sec^{-1}

An example of a "loose bolt" effect[17a] on internal conversion is available from data on the radiationless decay of alkyl benzenes.[22] For example, the fluorescence yield of toluene (**7**) is $\Phi_F \sim 0.14$, whereas the fluorescence yield of tert-butyl benzene (**8**) is $\Phi_F \sim 0.032$.

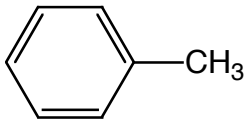

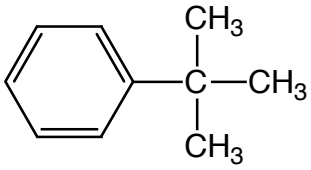

7 **8**

$k_{IC} \sim 10^7$ sec^{-1} $k_{IC} \sim 10^8$ sec^{-1}

It was shown that the mechanism for decrease in Φ_F was neither intersystem crossing nor photoreaction. It appears that the σ-bonds of the tert-butyl group serves as a "loose bolt" to accelerate internal conversion by a factor of ~10 (possibly via a mechanism related to Fig. 5.12a).

In addition, the observation that **7** is much more strongly phosphorescent (Φp^{REL} ~ 1.0) than **8** (Φ_P^{REL} ~ 0.00) at 77 K is probably a manifestation of the "loose bolt" effect on $T_1 \rightarrow S_1$ intersystem crossing.[23]

5.13 Radiationless Transitions between "Matching" or adiabatic surfaces

In Figure 5.2d a "matching" of two energy surfaces is shown. In this hypothetical case, the two surfaces are not related by a Zero Order surface crossing at r_c. Such surfaces, are essentially adiabatic surfaces and correspond to essentially pure "eigenstates" and possess wavefunctions Ψ_1 and Ψ_2 which are not strongly mixed. Thus there is no geometry at which the two surfaces approach the same energy. Is a radiationless transition between the two surfaces still plausible? The answer is positive because the longer lifetime of the state may make up for the weaker coupling. However, the qualification should be kept in mind that such radiationless transitions are expected to be much slower than those at critical geometries corresponding to situations (a), (b), (c) and (e) in Figure 5.2. In this case the representative point is viewed as residing in the minimum of the surface as it awaits a perturbation that will trigger the transition to the lower surface. Of course, if the time it takes for the perturbation to occur is too long, radiative transition from the upper to the lower surface may occur.

What determines the rate of transfer from an upper surface of the type shown in Figure 5.2d. From theory,[24] the rate of any transitions between vibrational states will be determined by the overlap of the vibrational wavefunctions, which is given by the *Franck-Condon factor* $f_v = \langle\chi_i|\chi_f\rangle^2$. The value of f_v in general follows the energy gap law given by eq. 5.17

$$f_v \sim \exp - \Delta E \qquad (5.17)$$

i.e., the rate of a radiationless transition from r_c (for a "matching") will fall exponentially as ΔE increases, if f_e and f_s are not rate-determining.

As an example of how the Franck-Condon factor operates to control the rate of spin-allowed processes corresponding to Figure 5.2d, consider internal conversion (f_s = 1). Suppose that two excited states S_2 and S_1 possess potential curves which undergo a Zero Order crossing at point F, but that the ground-state-potential curve is "matching" with (i.e., does not intersect in Zero Order) S_1 and S_2 (Fig. 5.13). A transition from S_2 to S_1 can occur without an appreciable alteration of position or momentum of the nuclei if the transition occurs at geometries near F, because the Franck-Condon factor is favorable near F. Such an internal conversion is expected to occur relatively rapidly. The direct radiationless transition $S_2 \rightarrow S_0$, however, is highly improbable, because the states do not have a crossing of surfaces.

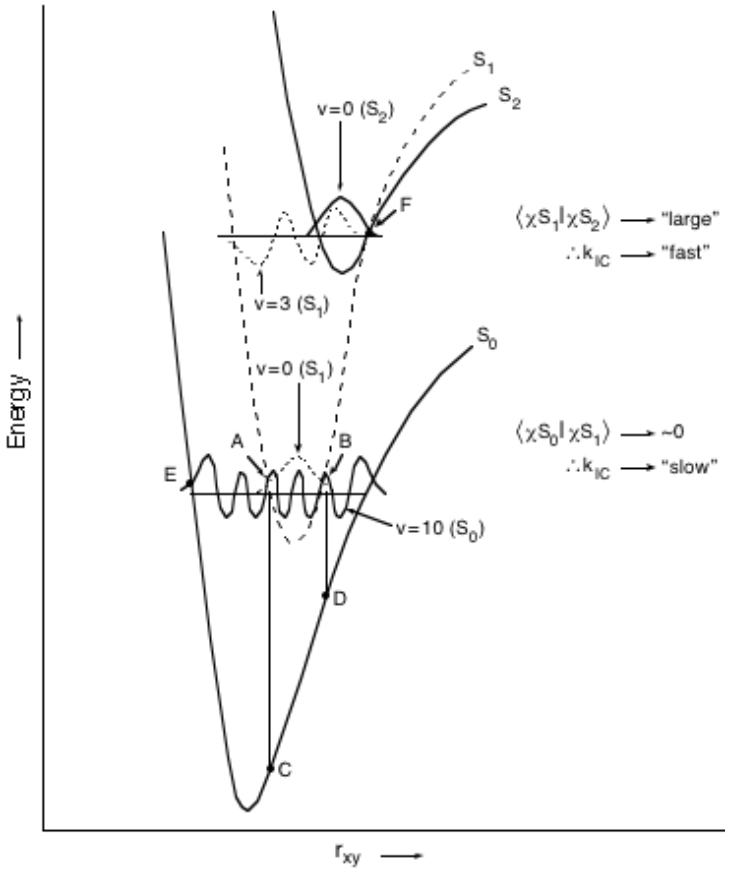

Figure 5.13 ***Representation of internal conversion between S_2 and S_1 and between S_1 and S_0.***

Now consider what happens when a molecule reaches the lowest vibrational levels of S_1. From Figure 5.13 it can be seen that if the vibrational eigenfunctions for χS_o (a high-energy vibrational level of S_0) oscillates rapidly from negative to positive values in the region where χS_1 (the $\nu = 0$ state of S_1) is always positive, then the overlap integral $<\chi S_1 \chi S_0>$ which determines the Franck-Condon factor will be very small making the $S_1 \rightarrow S_0$ transition rate very low. This contrasts with the situation in the region of interaction about point F. For this case, χS_1, and χS_2 (in the $\nu = 0$ state) are situated so the overlap integral $<$l $\chi S_2 \chi S_1>$ has a considerable value and the rate of internal conversion is relatively rapid. (The reader is referred to Sections 4.8, 4.12, and 4.13 for a review.) The $S_2 \rightarrow S_1$ transition is therefore, more rapid, and more probable than the $S_1 \rightarrow S_0$ transition, if the electronic part of the molecular wavefunctions for the two transitions are comparable.

As discussed above, organic compounds which possess rigid cyclic structures tend to fluoresce strongly (e.g., structures **3** and **4** discussed above). We may now theoretically rationalize this result from the standpoint of the Franck-Condon principle for radiationless transitions. The Franck-Condon principle tells us that for rigid structures the conversions $S_1 \rightarrow S_0$ and $T_1 \rightarrow S_0$ will be difficult, because the restraints placed on the molecule tend to hold the nuclei together. In effect, the S_1 states of such systems are constrained in their exploration of the excited surface as they seek to find "loose bolts," "free rotors," or intersystem crossing mechanisms. Thus, they fluoresce with high efficiency (e.g., **3** and **4**).

5.14 Factors that Influence the Rate of Vibrational Relaxation

The advent of pulsed picosecond and femtosecond laser spectroscopy has allowed the direct measurement of vibrational relaxation processes in fluid solutions at room temperature. For organic molecules[25] values of k_{vib} (rate constant for vibrational relaxation) are typically $\sim 10^{12}$-10^{14} sec^{-1}. Why is the transfer of excess vibrational energy to the environment so rapid? The answer is that both the vibrations within an

excited molecule and the environment have the ability to accept the energy of nuclear motion of a molecule and convert it into many different degrees of vibrational motion, Because the number of vibrational, rotational and translational energy levels of the environment is for all intents and purposes continuous, it may serve as a classical heat bath, capable of taking up any amount of vibrational energy which the excited molecule needs to dispose.[26]

Direct measurements of vibrational relaxation have been made for both the ground state or organic molecules and electronically excited states. The following qualitative observations can be summarized from the findings:

(1) For a given molecule vibrational relaxation occurs in two time domains. The first domain (typical range 10-0.1 ps, 10^{11}-10^{13} sec^{-1}) corresponds to ***intramolecular vibrational relaxation*** (IVR). The second domain (typically 1000-10 ps, 10^{9}-10^{11} sec^{-1}) corresponds to the vibrational energy transfer (VET(from the molecule to the solvent.

(2) Electronic relaxation is generally not rate limiting for IVR from S_n to S_1 (Kasha's rule).

(3) IVR is slightly faster in *R than in R.

A pictorial description of vibrational relaxation of an electronically and vibrationally excited molecule is shown in Figure 5.14 with formaldehyde in its equilibrated S_1 as a concrete example. In the excited state, the electron motion and position are responsible for the excess energy of the molecule, but the vibrations of S_1 are not excited and the local solvent molecules are "cool", i.e., their translational and vibrational motion is average in relation to the macroscopic temperature. Imagine that internal conversion (or intersystem crossing) occur from S_1, and that radiationless transition is promoted by the C=O vibrational coupling. This means that the electronic motion and position change (e → e) and the C=O vibration are coupled. Each of the transitions, $S_1 \rightarrow S_0$, $T_1 \rightarrow S_0$, after they occur isoenergetically, require excess vibrational energy to be dissipated somehow. Where does the energy to after the isoenergetic electronic transition has occurred? We imagine it to be dissipated as follows (Fig. 5.14): (1) The electronic transition from a π* orbital to a n orbital produces a "hot" C=O vibration. The vibrationally excited C=O group transfers some of its energy to the

C-H vibrations and some of its energy to the solvent. The excited vibrations of the formaldehyde "cool down" and the local microscopic temperature "heats up", i.e., the solvent molecules in the immediate vicinity of the formerly excited molecule have a higher translational and vibrational energy than the average for the macroscopic temperature for a brief period of time (1-10 picoseconds).

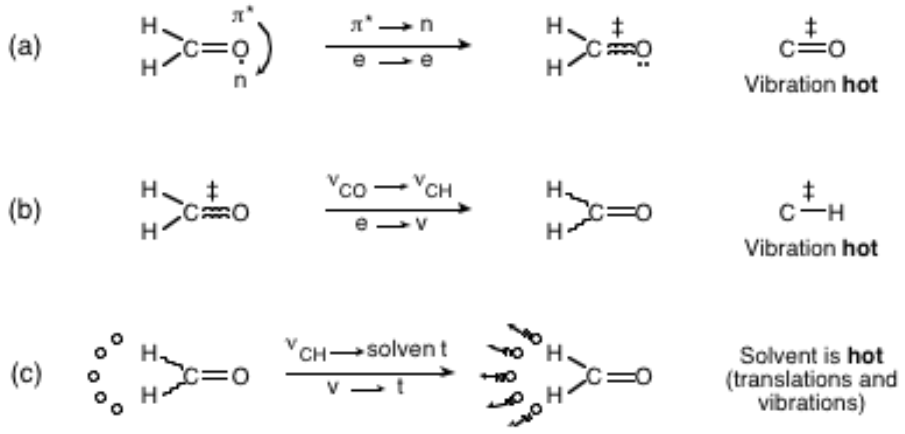

Figure 5.14 ***Schematic description of energy dissipation for formaldehyde. (a) the conversion of electronic excitation into vibration for formaldehyde, initially localized as excitation (wiggly lines) between the C and O atoms, followed by (b) vibrational energy transfer to the CH bonds, and (c) transfer to translational motion of the solvent.***

It appears that in fluid solution or in rigid matrices, the take-up of energy by the solvent is rarely if ever rate-determining for a radiationless transition.[26] One might ask at this point if emission of infra-red radiation is a significant path for transitions between the rotational and vibrational levels. Experimentally, infrared emission (loss of a few quanta at a time) does not compete with radiationless deactivation, but ultraviolet and visible emission do. This result follows theoretically from the relationship:[27]

$$k = 64\pi^4/3h \ \nu^3|H_{21}|^2 \ \alpha \ <H_{21}>^2 \qquad (5.18)$$

where v is the wave number of the photon which is emitted upon passing from state 2 to state 1, H_{21} is the electric dipole matrix element for the transition, (Section 5.3), and k is the rate constant for spontaneous emission.

Since v is 1,000 to 3,000 cm^{-1} for infrared transitions, while v ~ 30,000 cm^{-1} for ultraviolet transitions, the v^3 term places a prohibition factor of about 10^{-3} or greater on the relative rate of infrared emission as compared to ultraviolet-visible emission. Furthermore, the dipole-moment changes involved in pure vibrational transitions are usually small compared to those which occur upon passing from one electronic state to another. This factor may apply another order of magnitude prohibition on the rate of infrared emission.

In any case, the inherent rate constants for infrared emission are typically of the order of 10^2 sec^{-1} or smaller. For example,[28] an infrared emission of CO_2 occurs at ~1000 cm^{-1} and possesses a transition dipole of ~0.1 Debyes. This results in a k value of ~ 10^2 sec^{-1}. Since the rates of vibrational deactivation of molecules in solution[25] are of the order of 10^{12}-10^{13} sec^{-1}, we see that vibrational fluorescence will generally be a minor pathway for vibrational deactivation in condensed phases.

5.15 The Evaluation of Rate Constants for Radiationless Processes from Quantitative Emission Parameters

In general, a combination of experimental emission lifetimes τ_e and emission quantum yields Φ_e provides a convenient means of measuring the unimolecular rate constants of internal conversion (k_{IC}) and intersystem crossing (k_{ST} and k_{TS}). Knowledge of the rates of interconversions and lifetimes of excited states is of great importance in analyzing photochemical problems. The following scheme (5.19-5.24), based on the working state energy diagram of Fig. 1.3, lists all of the important unimolecular photophysical transitions that are expected to occur after absorption of light (5.19) and provides a means of estimating these rates from spectral data alone. The scheme assumes, for simplicity, the absence of irreversible photochemical reactions and specific bimolecular quenching. Such processes are readily included if desired.

	Step	**Rate**	
$h\nu + S_0 \rightarrow S_1$	Excitation	I	(5.19)

$S_1 \rightarrow S_0$ + heat	Internal conversion	$k_{IC}[S_1]$	(5.20)
$S_1 \rightarrow T_1$ + heat	Intersystem crossing	$k_{ST}[S_1]$	(5.21)
$T_1 \rightarrow S_0$ + heat	Intersystem crossing	$k_{TS}[T_1]$	(5.22)
$T_1 \rightarrow S_0 + h\nu$	Phosphorescence	$k_p^0[T_1]$	(5.23)
$S_1 \rightarrow S_0 + h\nu$	Fluorescence	$k_F^0[S_1]$	(5.24)

The steady-state approximation in excited singlet states assumes that the rate of absorption of photons (I) is equal to the total rate of deactivation of S_1 and leads to

$$I = (k_{ST} + k_F^0 + k_{IC})[S_1] \tag{5.25}$$

where I is the rate of absorption of light in einsteins/liter sec (photons/liter sec), and $[S_1]$ is the concentration of excited singlets. Similarly, the steady state approximation assumes that the rate of formation of triplets is equal to the total rate of deactivation of T_1, leading to eq. 5.26

$$k_{ST}[S_1] = k_{TS} + k_P^0)[T_1] \tag{5.26}$$

Transforming eq. 5.26 to solve for $[T_1]$ leads to eq. 5.27.

$$[T_1] = k_{ST}[S_1]/(k_P^0 + k_{TS}) \tag{5.27}$$

Under the conditions of steady-state excitation, the efficiency of a process from S_1 or T_1 is simply the ratio of the rates of the process of interest to the total deactivation rate of the state.

From the conventional state-energy diagram we can express the quantum yields, Φ, for transitions from each state as shown in eqs. 5.28-5.32:

$$\Phi_F = k_F^0/(k_F^0 + k_{ST} = k_{IC}) \tag{5.28}$$

$$\Phi_{IC} = k_{IC}/(k_F^0 + k_{ST} + k_{IC}) \quad (5.29)$$

$$\Phi_{ST} = k_{ST}/(k_F^0 + k_{ST} + k_{IC}) \quad (5.30)$$

$$\Phi_P = \Phi_{ST} \times k_P^0/(k_P^0 + k_{TS}) \quad (5.31)$$

$$\Phi_{TS} = \Phi_{ST} \times k_{TS}/(k_P^0 + k_{TS}) \quad (5.32)$$

For S_1, Φ_F is equal to the ratio of the rate of fluorescence to the total rate of deactivation of the S_1 state. Similarly, Φ_{ST} is equal to the ration of the rate of intersystem crossing to the total rate of deactivation of S_1. However, the Φ_P depends not only on the ratio of the rate of phosphorescence to the total deactivation rate of T_1, but also depends directly on Φ_{ST}, the probability that T_1 is formed from S_1. For example, if Φ_{ST} is zero, there can be no measurable phosphorescence upon direct excitation of S_1.

The singlet lifetime τ_s is equal to the inverse of the sum of all rates that deactivate S_1 (eq. 5.33) and the triplet lifetime τ_T is equal to the inverse of the sum of all rates that deactivate T_1, (eq. 5.34).

$$\tau_s = 1/(k_F^0 + k_{ST} + k_{IC}) \qquad \text{experimental } S_1 \text{ lifetime} \quad (5.33)$$

$$\tau_T = 1/(k_P^0 + k_{TS}) \qquad \text{experimental } T_1 \text{ lifetime} \quad (5.34)$$

Thus with the definition of the inherent radiative lifetimes $\tau_F^0 = (k_F^0)^{-1}$ and $\tau_P^0 = (k_P^0)^{-1}$ the expressions for quantum yields may be written as:

$$\Phi_F = k_F^0 \tau_S \quad (5.35)$$

$$\Phi_{IC} = k_{IC} \tau_S \quad (5.36)$$

$$\Phi_{ST} = k_{ST} \tau_S \quad (5.37)$$

$$\Phi_P = \Phi_{ST} k_P^0 \tau_T \quad (5.38)$$

$$\Phi_{TS} = \Phi_{ST} k_{TS} \tau_T \quad (5.39)$$

Experimentally, values of τ_S and τ_T may be evaluated directly by measurement of the decay of S_1 and T_1 as a function of time. In the case of S_1, the most convenient method to monitor $[S_1]$ is usually by measuring the fluorescence intensity emitted from S_1. Thus, τ_S is generally the same as the measured fluorescence lifetime, τ_F (not the pure radiative lifetime, τ_F^0). Similarly, measurement of the phosphorescence lifetime, τ_P, provides a direct measure of τ_T. In the case of triplet states, T_1 may be measured also by flash absorption spectroscopy (this method is discussed in detail in Chapter 8).

Measurement of Φ_f, Φ_p, Φ_{ST}, τ_s, and τ_T allow evaluation of the rate constants k_F^0, k_P^0, k_{IC}, k_{ST} and k_{TS}. The measurement of Φ_{ST} sometimes requires special methods.[29] For certain systems such as rigid aromatic hydrocarbons internal conversion from S_1 can be neglected $\Phi = 1 - \Phi_F$, i.e., every singlet which does not fluoresce is assumed to undergo intersystem crossing. The validity of this assumption depends on the absence of photoreactions, surface crossings or other quenching processes of S_1.

5.16 Examples of the Estimation of Rates of Photophysical Processes from Spectroscopic Emission Data.

As an example[30] of the calculation of radiationless rate constants from spectroscopic emission data, consider the state diagram for 1-chloronaphthalene (Fig. 5.15). At 77 K this molecule shows a weak ($\Phi_F = 0.06$) fluorescence but a strong ($\Phi_P = 0.54$) phosphorescence. The measured fluorescence and phosphorescence lifetimes are ~ 10×10^{-9} sec and 0.3 sec respectively.[30] Notice that 40% of the absorbed photons are not accounted for by emission ($\Phi_F + \Phi_P = 0.60$). We shall see in Section 5.9 that internal conversion ($S_1 \rightarrow S_0$) is not likely to compete with intersystem crossing (S_1 T_1) for a rigid aromatic molecule such as naphthalene. As a result, we may compute $\Phi_{ST} = 1 - 0.06 = 0.94$. Since $\Phi_{ST} = 0.94$ but Φ_P is only 0.54 we deduce that $\Phi_{TS} = \Phi_{ST} - \Phi_P = 0.40$.

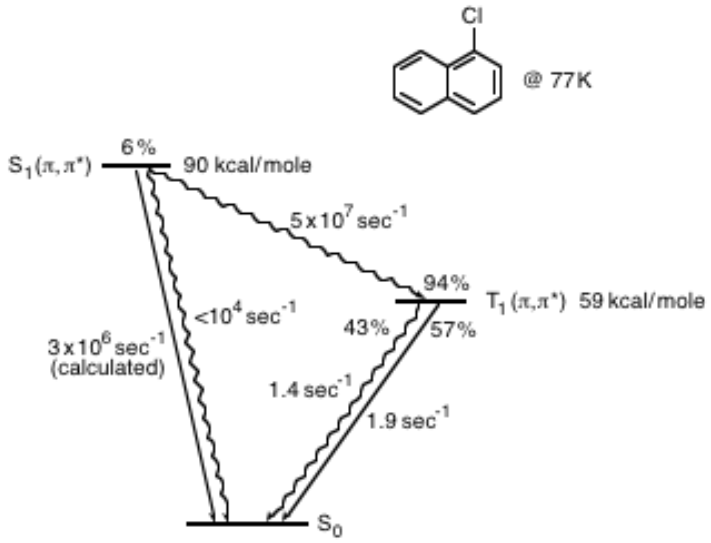

Figure 5.15 Energy diagram for 1-chloronaphthalene at 77 K, at 25° C, $k_t \sim 10^4$ sec^{-1}.

From these data and use of Eqs. 5.37 and 5.39 we find:

$$k_{ST} = \Phi_{ST}/\tau_S = 0.94/10^{-8} = 9.4 \times 10^7 \text{ sec}^{-1} \quad (5.40)$$

and,

$$k_{TS} = \Phi_{TS}/\Phi_{ST}\tau_T = 0.40/0.94)(0.3) = 1.4 \text{ sec}^{-1} \quad (5.41)$$

If k_{IC} is at least tem times smaller than the major rate determining deactivation pathway of S_1 (i.e., k_{ST}) we may estimate an upper limit to k_{IC} as:

$$k_{IC} < 0.1k_{ST} \text{ or } k_{IC} < 0.1k_F \quad (5.42)$$

The inherent or radiative rate constants for emission k_F^0 and k_P^0 may be calculated from Eqs. 5.35 and 5.38, i.e.,

$$k_F^0 = \Phi_F/\tau_S = 0.06/10^{-8} = 6 \times 10^6 \text{ sec}^{-1} \quad (5.43)$$

$$k_P^0 = \Phi_P/\Phi_{ST}\tau_P = 0.54/(0.94)(0.3) = 1.9 \text{ sec}^{-1} \quad (5.44)$$

As a second example, consider benzophenone (Fig. 5.16). This molecule is essentially non-fluorescent ($\Phi_F < 10^{-4}$) and possesses a very short singlet lifetime ($\tau_S \sim 10^{-11}$ sec). At 77 K, benzophenone^{31} shows a strong phosphorescence ($\Phi_P = 0.90$) with a lifetime of 6 x 10^{-3} sec. Since 90% of the photons absorbed by benzophenone are accounted for by phosphorescence, a maximum of 10% of the S_1 molecules can be undergoing $S_1 \rightarrow S_0$ internal conversion. In fact, it appears that nearly every molecule in S_1 undergoes intersystem crossing to T_1. In other words,

$$k_{ST} = \Phi_{ST}/\tau_S = 10^{11} \text{ sec}^{-1} \qquad (5.45)$$

This remarkably fast intersystem crossing rate is typical of certain carbonyl compounds possessing $S_1(n,\pi^*)$ states with a close lying $T(\pi,\pi^*)$ state.

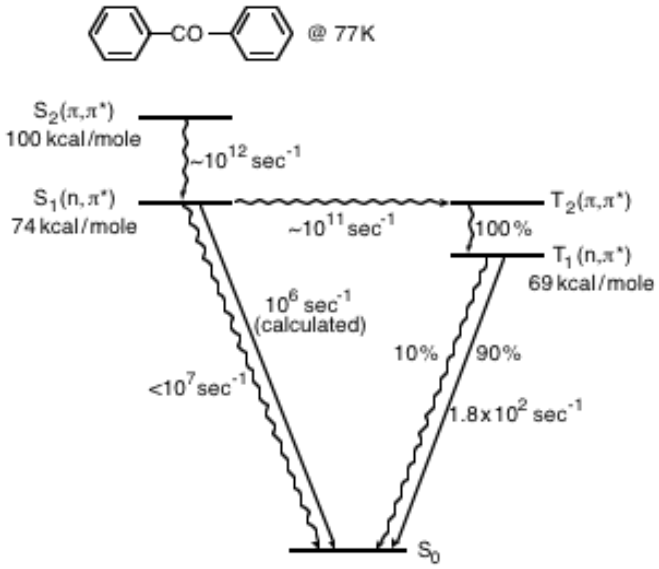

Figure 5.16 State diagram for benzophenone at 77 K.

The value of k_{TS} and k_P for benzophenone are given by:

$$k_{TS} = \Phi_{TS}/\Phi_{ST}\tau_T = 1.7 \text{ x } 10 \text{ sec}^{-1} \qquad (5.46)$$

$$k_P = \Phi_P/\Phi_{ST}\tau_T = 1.5 \text{ x } 10^2 \text{ sec}^{-1} \qquad (5.47)$$

If Φ_F is too weak to measure accurately, k_F may be determined indirectly, i.e., by application of the equation relating ε_{max} to τ_F (Eq. 5.23). The value of $\tau_F = 10^{-6}$ sec for the pure fluorescence rate of benzophenone is obtained in this manner.

Empirically, the oberved unimolecular rate constant for a radiationless transition k_{OB} may be considered to be composed of temperature-independent and temperature-dependent components, i.e.,

$$k_{OB} = k_{OB}^{0}(\text{T independent}) + k_{OB}(\text{T dependent}) \qquad (5.48)$$

The temperature-independent part of k_{OB} may be viewed as due to radiationless transitions that occur during the zero point motion of the molecule. Such transitions occur even at temperatures approaching O K! The temperature dependent part of k_{OB} may be viewed as due to radiationless transitions that require an activation energy. Such transitions usually obey an Arrhenius relationship (See Section 5.9 for examples).

5.17 Internal Conversion ($S_n \rightarrow S_1$, $S_1 \rightarrow S_0$, $T_n \rightarrow T_1$)

The three most important classes of internal conversion commonly encountered for organic molecules are:

1. Radiationless transition from an upper excited singlet state to the lowest excited singlet state, $S_n \rightarrow S_1$ (rate constant = k_{IC}^{SS});

2. Radiationless transition from an upper excited triplet state to the lowest lying triplet state, $T_n \rightarrow T_1$ (rate constant = k_{IC}^{TT});

3. Radiationless transitions from the lowest energy singlet state to the ground singlet state, $S_1 \rightarrow S_0$ (rate constant = k_{IC}).

We now present some examples of internal conversions and discuss the relationship of the rate of internal conversion to the structures of electronically excited states.

5.18 The Relationship of Internal Conversion to Excited State Structure of *R

Let us consider some experimental information concerning internal conversion in aromatic hydrocarbons. We begin with data taken at 77 K in a rigid glass matrix. Under these conditions photoreactions and bimolecular quenching may generally be completely avoided and fluorescence and phosphorescence are readily observed with significant quantum yields. Table 5.2 summarizes some pertinent data for the quantum yields of fluorescence (Φ_F), intersystem crossing (Φ_{ST}) and the energy of the lowest singlet (E_{S1}). The following two sweeping generalizations have been noted for rigid aromatic hydrocarbons and serve as a basis for discussion:[32]

1. Fluorescence occurs only from S_1 to S_0; phosphorescence occurs only from T_1 to S_0; S_n and T_n emissions are extremely rare (Kasha's rule).

2. The quantum yield of fluorescence and the quantum yield of phosphorescence are independent of initial excitation energy (Vavilov's rule).

Both of these rules result from the general very fast internal conversion from upper electronically excited states and very fast vibrational relaxation (10^{12}-10^{13} s^{-1}) within an electronically state ($S_n \rightarrow S_1$ and $T_n \rightarrow T_1$ processes). On the other hand, internal conversion from $S_1 \rightarrow S_0$ is much slower and molecules that are relatively rigid due to structures of environment cannot compete with fluorescence and intersystem crossing. Let us now see how such a conclusion may be deduced from experimental data. The lack of measurable fluorescence from $S_n(n > 1)$ means that emission yields from these states are less than 10^{-4}. From the value of the extinction

Table 5.2 Quantum Yields for Fluorescence and Intersystem Crossing of Organic Molecules[a]

Molecule (Configuration of S_1)	Φ_F	Φ_{ST}	$1-(\Phi_F + \Phi_{ST})$[b]	E_{S_1}[c]
Benzene (π,π^*)	0.05	0.25	0.70	110
1,3-Dimethylbenzene (π,π^*)[d]	0.35	0.65	<0.05	100
Naphthalene (π,π^*)	0.20	0.80	<0.05	92
Anthracene (π,π^*)	0.70	0.30	<0.05	76
Tetracene (π,π^*)	0.15	0.65	0.20	60
Pentacene (π,π^*)	0.10	0.15	0.75	50
Azulene (π,π^*)	0.000	---	Low	50
Acetone (π,π^*)	0.001	~1.0	0.05	85
Biacetyl (n,π^*)	0.002	~1.0	0.05	65
Benzophenone (n,π^*)	0.000	~1.0	0.05	75
5-Methyl-2-heptanone (n,π^*)[e]	0.000	0.10	0.90	85
Cyclobutanone (n,π^*)[f]	0.000	0.00	1.0	80
1,3-Pentadiene (n,π^*)[g]	0.000	0.00	1.0	100

[a] Except where noted, data for molecules in fluid solution at room temperature from Wilkinson, F., *Organic Molecular Photophysics*, ed. Birks, J.B., New York: Wiley, 1075, p. 95.

[b] A lower limit of 5% is placed on the experimental uncertainty of measurements of Φ. This quantity sets an upper limit to Φ_{IC}.

[c] Singlet energy (0,0 energy) in kcal/mole.

[d] Carroll, F.A., and Quinta, F.H., *J. Am. Chem. Soc.*, *98*, 1 (1976).

[e] Yang, N.C., and Elliott, S.P., *J. Am. Chem. Soc., 91*, 7550 (1969). Reaction ($\Phi \sim 0.05$) occurs in S_1. See Chapters 8 and 10.

[f] Morton, D.R., and Turro, N.J., *Adv. Photochem., 9,* 197 (1974). A cleavage reaction occurs with an efficiency of ~0.3 from S_1.

[g] Srinivasan, R., *J. Am. Chem. Soc., 84*, 4141 (1962). In Chapters 11 and 12, it will be shown that $\Phi_{ST} \sim 0$ in general for simple ethylenes and polyenes. An isomerization reaction of efficiency ~ 0.1 from S.

coefficient $S_0 \rightarrow S_n$ we may estimate the radiative rate constant for $S_n \rightarrow S_0$. Knowledge of this rate and a limit of Φ_F allow us to calculate a limit for the radiationless rate $S_n \rightarrow S_1$.

Consider anthracene as an example to estimate the rate of internal conversion from upper excited singlet states. From eq. 5.23, we can estimate the rate of fluorsece from upper singlet states, even those such fluorescence is not observed experimentally. From example, the $S_0 \rightarrow S_3$ absorption maximizes at 39,700 cm^{-1} (252 nm) with $\varepsilon_{max} \sim 2 \times 10^5$. From Eq. 5.23:

$$k_F^0 \sim 2 \times 10^9 \qquad (5.49)$$

Since

$$\Phi_F^{S_2} = k_F^0/k_D < 10^{-4} \qquad (5.50)$$

$$k_D > 10^4 k_F \sim 2 \times 10^{13}\ sec^{-1} \qquad (5.51)$$

In other words, S_3 deactivates to S_1 with a rate constant of the order of that for vibrational motion. Since *emission* from S_1 is observed when S_3 of anthracene is excited, we must conclude that $k_{IC}(S_3 \rightarrow S_1) \sim 10^{13}\ sec^{-1}$. It appears that for most organic molecules $k_{IC}(S_n \rightarrow S_1)$ falls in the range 10^{11}-$10^{13}\ sec^{-1}$. Evidently, electronic relaxation by internal conversion from upper levels is rate-limited by only nuclear

vibrational motion. This in turn suggests that Zero Order crossings are common for S_n(n >1) states and that critical geometries may be readily achieved during vibrational motion of S_n in its $\nu = 0$ level.

Because the fluorescence quantum yield for anthracene is significant ($\Phi_F \sim 0.7$) from S_1, the $S_1 \rightarrow S_0$ internal conversion must, at best, be competitive only with other modes of decay from S_1. In Table 5.2 we noted that at 77K, $\Phi_F + \Phi_{ST} \sim 1$ for many aromatic hydrocarbons possessing rigid structures. As a result, the internal conversion $S_1 \rightarrow S_0$ cannot occur to more than a few percent (the experimental error of measuring Φ) for these compounds.

For example,[32] since the singlet decay of pyrene is $\sim 10^6$ sec^{-1} and since $\Phi_F + \Phi_{ST} \sim 1.00$, we must conclude that $k_{IC}(S_1 \rightarrow S_0) < 10^6$ sec^{-1}. Thus, a factor of $\sim 10^6$ separates the typical rate of a $S_n \rightarrow S_1$ internal conversion from a typical $S_1 \rightarrow S_0$ internal conversion.

Relatively little data exist on the direct measurement of the rates of $T_n \rightarrow T_1$ internal conversions. The reason for this lack of data may be technical rather than theoretical in nature. One would expect that $T_2 \rightarrow T_1$ *fluorescence* should occur with a *range* of efficiencies as does $S_1 \rightarrow S_0$ fluorescence. However, $T_2 \rightarrow T_1$ energy gaps generally are on the order of 30 kcal/mole or *smaller*. This means that $T_2 \rightarrow T_1$ fluorescence, even if it occurs efficiently would appear at wavelengths greater than ~800 nm. Experimentally, however, equipment capable of measuring light at these wavelengths with high sensitivity is not available.

In favorable cases, however, a very weak $T_2 \rightarrow T_1$ fluorescence has been observed. For example,[33] 9,10-dibromoanthrocene displays a weak ($\Phi_F \sim 10^{-6}$) $T_2 \rightarrow T_1$ fluorescence. From the extinction coefficient for $T_1 \rightarrow T_2$ absorption, $k_F(T_2 \rightarrow T_1)$ can be derived and it is found that $k_F \sim 10^5$ sec^{-1}. From the value of Φ_F and Eq. 5.27 we deduce that $k_{IC}(T_2 \rightarrow T_1) \sim 10^{11}$ sec^{-1}, a very reasonable value considering the rather large energy gap between the interconverting states. Indirect evidence also supports a value of k_{IC} of $\sim 10^{11}$ sec^{-1} for 9,10-dibromoanthracene.[34]

5.19 The Energy Gap Law for Internal Conversion ($S_1 \rightarrow S_0$)

In the absence of a Zero Order surface crossing between S_1 and S_0 a $S_1 \rightarrow S_0$ internal conversion must occur via a "Franck-Condon forbidden" mechanism, i.e., the nuclei in one state must undergo a rather drastic change in position and momentum as a result of the transition, since the net overlap of vibrational wave-functions in both states is small.[24,35] For such situations the $S_1 \rightarrow S_0$ internal conversion is often rate limited by the Franck-Condon factor, $\langle\chi|\chi\rangle^2 = f_v$. If we take 10^{13} sec^{-1} as an order-of-magnitude estimate of the maximum rate of internal conversion, then from Eq. 5.5

$$k_{IC} \sim 10^{13} f_v \qquad (5.52)$$

It is possible to calculate or estimate f_v from spectral data.[36] Both theoretical and experimental evidence demonstrate that f_v is a very sensitive function of the *energy gap*, ΔE, between the zero point vibrational levels of the states undergoing internal conversion.[35] From Eq. 5.17 and Eq. 5.52:

$$k_{IC} \sim 10^{13} \exp - \alpha\Delta E \qquad (5.53)$$

where α is a proportionality constant. The energy gap law can be attributed to the changes in the Franck-Condon overlaps of the nuclear wavefunctions, which become increasingly unfavorable (at an exponential rate) with increasing energy separation.

Experimentally, $S_1 \rightarrow S_0$ internal conversion is usually negligible relative to fluorescence or intersystem crossing for non-photoreactive, relatively rigid molecules if $\Delta E(S_1 \rightarrow S_0)$ is larger than ~50 kcal/mole. For example, at $\Delta E \sim 100$ kcal/mole, $f_v \sim 10^{-8}$, so that $k_{IC} \sim 10^5$ sec^{-1}. Even for $\Delta E \sim 50$-60 kcal/mole, $f_v \sim 10^{-5}$ so that $k_{IC} \sim 10^8$ sec^{-1}. Since the *slowest* rates of $S_1 \rightarrow S_0$ fluorescence are generally $> 10^6$ sec^{-1}, and since the slowest rates of $S_1 \rightarrow T_1$ intersystem crossing are generally $>10^6$ sec^{-1}, we see that

internal conversion is unlikely to compete favorably with fluorescence or intersystem crossing if $\Delta E(S_1 \rightarrow S_0)$ is >50 kcal/mole.

Thus, we have a theoretical basis for Ermolev's rule that: [37]

$$\Phi_F + \Phi_{ST} = 1 \text{ because } 1 - (\Phi_F + \Phi_{ST}) \sim \Phi_{IC} \qquad (5.54)$$

For example, tetracene and pentacene (Table 5.2) possess relatively low singlet energies (~60 and ~50 kcal/mole, respectively) and undergo significant internal conversion from S_1 ($\Phi_{IC} \sim 0.20$ ad 0.75, respectively). The large value of Φ_{IC} for benzene (0.80) is probably due to a reversible photoreaction or a surface crossing of the S_1 and S_0 surfaces. In the case of the last three entries of Table 5.2 (5-methyl-2-heptanone, cyclobutanone, and 1,3-pentadiene) reversible photochemical reaction from S_1 probably accounts for a significant fraction of Φ_{IC}.

5.20 The Deuterium Isotope Test for Internal Conversion

An "isotope test" for the origin of the energy gap law of Eq. 5.51 is available. The Franck-Condon factors are generally *greatest* for high frequency vibrations.[24,35] This is because the higher the energy of a vibration the fewer the number of quanta required to match an electronic gap with vibrational energy. The highest frequency vibrations in organic molecules (Table 5.1) often correspond to C-H stretching motions (~3000 cm^{-1}). We thus expect that electronic-vibrational energy transfer will be fastest for "leakage" through C-H vibrations. If C-H vibrations are replaced by lower energy C-D vibrations (~2200 cm^{-1}) the rate of electronic to vibrational energy transfer should be slowed down substantially. Thus, we predict that if $S_1 \rightarrow S_0$ occurs via an electronic-vibronic mechanism, the lifetime of $S_1(\tau_s)$ will be *increased* by the substitution of C-D for C-H, because k_{IC} will decrease (Eq. 5.33). Thus, we have an *isotope test* for internal conversion.

Experimentally, the replacement of C-H bonds by C-D bonds in aromatic hydrocarbons[38] generally does not change the singlet state lifetime or the fluorescence yield. For example, [38c] at 77 K both pyrene-h_{10} and pyrene-d_{10} possess a fluorescence yield of 0.90, and singlet lifetimes (τ_s) of 450 ns. Since $\tau_s = (k_F = k_{ST} + k_{IC})\text{-}1$ and since τ_s (pyrene-h_{10}) = τ_s(pyrene-d_{10}), we may conclude $k_F = k_{ST} >> k_{IC}$, because a large decrease in k_{IC} is expected upon going from the h_{10} to d_{10} compound. The important point to be made here is that since there is no significant deuterium isotope effect on τ_s or Φ_F, internal conversion ($S_1 \rightarrow S_0$) cannot contribute significantly to the decay of S_1. In Section 5.10 we shall see that a large deuterium effect does operate on $T_1 \rightarrow S_0$ intersystem crossing.

In contrast to the small influence of the substitution of D for H on ts and Φ_F for aromatic hydrocarbons, this substitution may cause a significant enhancement for ketones and aldehydes. The effect of deuteration on Φ_F is most dramatic for aldehydes, especially in the vapor phase.[39]

For example,[39] the fluorescence quantum yield of formaldehyde increases by a factor of ~20 upon going from $H_2C{=}O$ to $D_2C{=}O$.

$H_2C{=}O$	$D_2C{=}O$	Low pressure vapor phase
	Φ_F~0.4	
	τ_s	~0.08 μs

Evidently, the substitution of D for H greatly decreases the magnitude of k_{ST} or k_{IC}. It is not yet clear whether a spin-orbit or Franck-Condon inhibition is involved.

The effect of deuteration on acetone[40] is less striking (τ_s acetone-h_6 is 1.17 ns, acetone-d_6 is 2.3 ns), it is nonetheless significant. In this case it appears that intersystem crossing may be specifically slowed down by deuteration, possibly because of a decrease of f_v upon deuteration.

5.21 Examples of Unusually Slow $S_n \rightarrow S_1$ Internal Conversion

Azulene[41] and its derivatives provide a striking exception to the general rule that $S_2 \rightarrow S_1$ internal conversion completely dominates fluorescence (in condensed phases). For azulene (**9**) Φ_F is ~ 0.03 (see Section 5.14). For some fluorinated derivatives the value of Φ_F for $S_2 \rightarrow S_0$ fluorescence is ~ 0.2! The rate of internal conversion ($S_2 \rightarrow S_1$) is exceptionally slow ($k_{IC} \sim 7 \times 10^8$ sec^{-1}) for **9**. This fact is consistent with the exceptionally large energy gap of ~40 kcal/mole between the 0,0 levels of S_2 and S_1 of azulene (Eq. 5.51), i.e., the $S_2 \rightarrow S_1$ internal conversion possess a poor Franck-Condon factor (Eq. 5.50).

Azulene structure

Azulene and its derivative are also remarkable for their exceptionally rapid rate of $S_1 \rightarrow S_0$ internal conversion (Table 5.2). Direct measurements[43] indicate that $k_{IC}(S_1 \rightarrow S_0)$ is ~ 10^{12}sec^{-1}. Such a large rate constant is consistent with a small value of E_{S1} and/or a surface crossing of the S_1 and S_0 surfaces near the $\nu = 0$ level of S_1.

5.22 Intersystem Crossing from S_1 to T_1

Table 5.3 presents some examples of the "spread", for exemplar organic molecules, of measured values of k_{ST} the rate constant for intersystem crossing from S_1 to T_1. First it should be noted that the smallest values of k_{ST} (~10^6 sec^{-1}) occur for aromatic hydrocarbons (pyrene, naphthalene), and the largest values (~10^{10}-10^{11} sec^{-1}) occur for molecules containing "heavy atoms," such as bromonaphthalene, or possessing $S_1(n,\pi^*)$ states that can mix effectively with $T_n(\pi,\pi^*)$ states such as benzophenone. However, it is clear that other factors in addition to the "heavy atom" or "n,π*" effects must also influence the value of k_{ST}. These factors are:

1. The energy gap, ΔE_{ST}, between S_1 and the state to which intersystem crossing actually occurs (i.e., T_1 or some *upper* triplet, T_n),

2. The electronic configurations of the states undergoing intersystem crossing.

The $S_1 \rightarrow T_1$ transition may occur via (a) direct spin-orbit coupling of S_1 to the upper vibrational levels of T_1, or (b) via spin-orbit coupling of S_1 to an upper T_n state followed by rapid $T_n \rightarrow T_1$ internal conversion.

For case 1 we expect the measured value of k_{ST} to depend on the energy gap between S_1 and T_1, whereas for case 2 the energy gap between S_1 and T_1 should not be significant. In addition to the singlet-triplet energy gap we expect that vibrational motion in the S_1 state is required to allow the molecule to explore different shapes as it searches for an effective spin-orbit coupling mechanism.

5.23 The Relationship between $S_1 \rightarrow T_1$ Intersystem Crossing to Molecular Structure

An important empirical observation (Table 5.3) is that at 77 K, nearly *all* measured values of k_{ST} for aromatic hydrocarbons fall in the range $\sim 10^8$-10^6 sec^{-1}. This range of rates is comparable to that of fluorescence, i.e., k_F^0 from aromatic hydrocarbons, $\sim 10^6$-10^9 sec. As a result, most aromatic hydrocarbons exhibit a measurable amount of fluorescence, and undergo significant intersystem crossing if k_F^0 is not maximal at low temperatures in a rigid medium.

To exemplify how these factors operate, let us compare the values of k_{ST} for the aromatic hydrocarbons anthracene[44] and pyrene.[45] In each case, an $S_1(\pi,\pi^*) \rightarrow T_n(\pi,\pi^*)$ process occurs. However, a variation factor of ~100 is noted in the rate of k_{ST}. The possibilities for this variation are (a) differing degrees of electronic coupling between S_1 and the triplet state to which crossing occurs, (b) differing energy gaps between S_1 and the triplet state to which crossing occurs, and (c) differing degrees of spin-orbit coupling between S_1 and the triplet state to which crossing occurs. The variation may be

---

Table 5.3 Representative Values of Intersystem Crossing Rates ($S_1 \rightarrow T_1$), Singlet-Triplet Energy Gaps.[a]

Molecule	$k_{ST}(sec^{-1})$[a]	ΔE_{ST} (kcal/mole)[a]	Transition
Naphthalene	10^6	30	$S_1(\pi,\pi^*) \rightarrow T_1(\pi,\pi^*)$
Anthracene	10^8	2-3	$S_1(\pi,\pi^*) \rightarrow T_2(\pi,\pi^*)$
Pyrene	10^6	30	$S_1(\pi,\pi^*) \rightarrow T_1(\pi,\pi^*)$
Triphenylee	5×10^7	30	$S_1(\pi,\pi^*) \rightarrow T_1(\pi,\pi^*)$
1-Bromonaphthalene	10^9	30	$S_1(\pi,\pi^*) \rightarrow T_1(\pi,\pi^*)$
9-Acetoanthracene[b]	$\sim 10^{10}$	~5	$S_1(\pi,\pi^*) \rightarrow T_2(n,\pi^*)$
Perylene	$<10^8$	~30	$S_1(\pi,\pi^*) \rightarrow T_1(\pi,\pi^*)$
3-Bromoperylene[c]	$<10^8$	30	$S_1(\pi,\pi^*) \rightarrow T_1(\pi,\pi^*)$
Acetone[d]	5×10^8	5	$S_1(n,\pi^*) \rightarrow T_1(n,\pi^*)$
Benzophenone[e]	10^{11}	5	$S_1(n,\pi^*) \rightarrow T_2(\pi,\pi^*)$
Benzil	5×10^8	5	$S_1(n,\pi^*) \rightarrow T_1(n,\pi^*)$
Biacetyl	7×10^7	5	$S_1(n,\pi^* \rightarrow T_1(n,\pi^*)$
9,10-Dibromo-anthracene[f]	$\sim 10^8$	30	$S_1(\pi,\pi^*) \rightarrow T_1(\pi,\pi*)$
		5 ???	$S_1(\pi,\pi^* \rightarrow T_2(\pi,\pi^*)$
[2.2.2]-diaza-bicyclo-octane[g]	$\sim 10^6$	25	$S_1(n,\pi^*) \rightarrow T_1(n,\pi^*)$

[a] Unless specified, data from Birks, J.B., *Photophysics of Aromatic Molecules*, New York: Wiley, 1970; or Wilkinson, F., *Organic Molecular Photophysics*, vol. 2, ed. Birks, J.B., New York: Wiley, 1975, p. 95. The values ΔE_{ST} (kcal/mole) refer to the energy gaps between S_1 and the triplet to which intersystem crossing occurs.

[b] Reference 42.

[c] Reference 36b.

[d] Reference 32a.

[e] Reference 13

[f] Reference 37

[g] Reference 40.

qualitatively explained on the basis of (c) alone. In the case of pyrene[45] it appears that S_1 crosses directly to an excited vibrational level of T_1. The energy gap $\Delta E_{ST} \sim 30$ kcal/mole. In the case of anthracene and substituted anthracenes,[46] S_1 may cross to T_2, which is nearly isoenergetic[49] with S_1. Thus, in anthracene a small energy gap and consequently a favorable Franck-Condon factor exists for intersystem crossing. Because the energy gap between S_1 and T_2 of anthracene is very small, substituents on the anthracene and solvent effects on a given anthracene can cause significant variations in quantum yield of fluorescence even thought the radiative rate of fluorescence does not change significantly with structural variations or solvent. The reason for the wide variation is that k_{ST} varies significantly, whereas k_F remains constant. (Give some more examples)

According to theory,[47] mixing of π,σ^* and σ,π^* triplet states with $S_1(\pi,\pi^*)$ is required to produce spin-orbit coupling and thereby imbue S_1 of aromatic hydrocarbons with "triplet character". This mixing must be vibronically induced so that mixing is relatively ineffective for molecules possessing a rigid structure in S_1.

With respect to n,π^* states, a similar situation appears to hold with respect to k_{ST} and the energy gap when $S_1(n,\pi^*) \rightarrow T_1(n,\pi^*)$ transitions (forbidden by El-Sayed's rule, Fig. 5.8) are involved. Recall that $S_1(n,\pi^*) \rightarrow T_1(n,\pi^*)$ do not generate spin orbit coupling in Zero order. Thus, both acetone ($k_{ST} = 5 \times 10^8$ sec^{-1})[48] and biacetyl ($k_{ST}=1 \times 10^8$ sec^{-1})[49] involve "forbidden" spin-orbit mechanisms but enjoy a small (~6 kcal/mole) ΔE_{ST} and (presumably) a favorable Franck-Condon factor. Simple aliphatic ketones possess a significantly forbidden fluorescence ($k \sim 10^5$ sec^{-1}). The net result is for aliphatic ketones typically $k_{ST} >> k_F$ and as a result $\Phi_{ST} \sim 1$ (Table 5.3). However, cyclic azoalkanes[50] which possess a large energy gap between S_1 and T_1 ($\Delta E_{ST} \sim 25$ kcal/mole) encounter a poorer Franck-Condon factor and k_{ST} is thereby considerably

slower. As a result, some cyclic azoalkanes exhibit a very high Φ_F because of a very small value of k_{ST}.in spite of a relatively slow rate of intersystem crossing.

The largest values of k_{ST} for organic molecules not possessing "heavy atoms" are found for systems undergoing $n,\pi^* \rightarrow \pi,\pi^*$ transitions (allowed by El-Sayed's rule, Fig. 5.8) with small energy gaps, e.g., benzophenone[13,51] ($k_{ST} = 10^{11}$ sec^{-1}, $^1n,\pi^* \rightarrow {}^3\pi,\pi^*$) and 9-benzoyl anthracene[52] ($k_{ST} = 10^{10}$ sec^{-1}, $^1\pi,\pi^* \rightarrow {}^3n,\pi^*$).

The magnitudes of k_{ST} for alkyl ketones is sensitive to molecular structure. For example, for acetone[48] $k_{ST} \sim 5 \times 10^8$ sec^{-1}, whereas for di-tert-butyl ketone[53] $k_{ST} \sim 10^8$ sec^{-1} and for perfluoroacetone[48] $k_{ST} \sim 10^7$ sec^{-1}. This variation suggests a decreasing amount of spin-orbit coupling or decreasing Franck-Condon factor as one proceeds from acetone to tert-butyl ketone to perfluoroacetone. The observation of a deuterium isotope effect[40] on k_{ST} and the rather large influence of substitution of fluorine are consistent with reduced Franck-Condon factors. The effect of "heavy atoms": on $S_1 \rightarrow T$ intersystem crossing is discussed in Section 5.11.

5.24 Temperature Dependence of $S_1 \rightarrow T$ Intersystem Crossing

The fluorescence yield Φ_F and singlet lifetimes τ_s of organic molecules are sometimes found to vary with temperature. Since k_F^0 is generally temperature independent,[32] some radiationless process from S_1 is temperature dependent. Indeed, photoreactions from S_1 commonly have small energy barriers and therefore will possess temperature dependent rate constants. Intersystem crossing ($S_1 \rightarrow T$) or internal conversion ($S_1 \rightarrow S_0$) may be temperature dependent if upper vibrational levels of S_1 possess a different mechanism for radiationless transition than the ν=0 level.

For example, the rate constant for intersystem crossing can be expressed as

$$k_{ST}^{OB} = k_{ST}^0 + A \exp - E/RT \qquad (5.55)$$

Experimentally, k_{ST}^{OB}, the observed rate constant, is sometimes found to be essentially temperature independent below a certain temperature and to follow Eq. 5.55 above that temperature. A common mechanism for this temperature dependence is thermally activated $S_1 \rightarrow T_n (n \neq 1)$ intersystem crossing.

The rate of intersystem crossing in certain anthracene derivatives is temperature dependent.[46] This observation has been explained in terms of a temperature dependent rate of intersystem crossing from S_1 to T_2. For example, the value of k_{ST} for 9,10-dibromoanthracene may be expressed as $k_{ST} \sim 10^{12} \exp - E_a/RT$ where $E_a \sim 4.5$ kcal/mole. A large energy gap between S_1 and T_1 serves to slow down the direct $S_1 \rightarrow T_1$ intersystem crossing because of an unfavorable Franck-Condon factor. That T_2 is populated, rather than an upper vibration level of T_1, is supported by triplet-triplet absorption measurements, which demonstrated that T_2 lies about 4-5 kcal/mole above S_1. Since the value of E_a is ~4.5 kcal/mole, it is logical to suppose that an activated $S_1 \rightarrow T_2$ process is involved in the temperature dependent intersystem crossing of 9,10-dibromoanthracene.

It is interesting to note that Φ_F and τ_s are usually not very temperature dependent below ~100 K. For example,[54] Φ_F of naphthalene is ~0.3 at both 77 K and at 4K. This implies that k_{ST} ($S_1 \rightarrow T$) is temperature independent in the range 4K to 77K. This result suggests that the energy term in Eq. 5.55 becomes small relative to k_{ST}^0 at temperatures below 100 K.

5.25 Intersystem Crossing ($T_1 \rightarrow S_0$)

Of the three important radiationless processes, $S_1 \rightarrow S_0$, $S_1 \rightarrow T_1$, and $T_1 \rightarrow S_0$, only in the latter case does no electronic states lie between the initial and final states, T_1 and S_0. Thus, phosphorescence and intersystem crossing are both derived from a common electronic $T_1 \rightarrow S_0$ transition.

5.26 The Relationship between $T_1 \rightarrow S_0$ Intersystem Crossing and Molecular Structure

As in the case of $S_1 \rightarrow S_0$ internal conversion, we expect an energy gap law (Eq. 5.17) and deuterium isotope effect if $T_1 \rightarrow S_0$ occurs via an electronic-vibrational (matching) mechanism. In addition, spin-orbit coupling may be important. It is not *a priori* obvious whether Franck-Condon factors (f_v) or spin-orbit factors ($f_{s)}$ will determine the ultimate k_{TS} value.

For aromatic hydrocarbons, a clear cut relationship between k_{ST} and (T_1) is found.[35] As for the $S_1 \rightarrow S_0$ process, we expect the high-frequency C-H vibrations to serve as the major "acceptor" vibrations for leakage of electronic into vibrational energy.[24] Indeed, a plot of log k_{ST} versus E(T_1) (corrected for the number of C-H vibrations) is linear.[35] This result provides strong evidence that the electronic energy of T_1 "leaks out" via C-H vibrations for rigid aromatic hydrocarbon

Factors other than Franck-Condon factors can influence the value of k_{ST} (Table 5.4). For example, increased spin-orbit coupling due to the heavy atom effect or the occurrence of an $^3n,\pi^* \rightarrow S_0$ transition will enhance the value of k_{TS}. Thus, for naphthalene, $k_{TS} \sim 0.4$ sec^{-1}, while for 1-bromonaphthalene $k_{TS} \sim 100$ sec^{-1}. Ketones possessing $T_1(n,\pi^*)$ undergo the fastest $T \rightarrow S_0$ crossings which have yet been measured ($k_{TS} \sim 10^3$ sec^{-1}) for organic molecules which don't possess heave atoms.

5.27 Deuterium Isotope Effects on $T_1 \rightarrow S_0$ Intersystem Crossing

Dramatic deuterium isotope effects are found for radiationless $T_1 \rightarrow S_0$ transitions,[24,35] results which contrast sharply with those for $S_1 \rightarrow T_1$ transitions. Presumably, the difference lies in the much smaller energy gap

---

Table 5.4 Some Representative Values of Triplet Energies, Phosphorescence Radiativer Rates, Intersystem Crossing Rates ($T_1 \rightarrow S_0$), and Phosphorescence Yields[a]

Molecule[b]	E_T	k_P^0	k_{TS}	Φ_P
Benzene-h_6	85	~0.03	0.03	0.20
Benzene-d_6	85	~0.03	<0.001	~0.80
Naphthalene-h_8	60	~0.03	0.4	0.05
Naphthalene-d_8	60	~0.03	<0.01	~0.80
$(CH_3)_2C=O$	78	~50	1.8×10^3	0.043
$(CD_3)_2C=O$	78	~50	0.6×10^3	0.10

[a] In organic solvents at 77 K. E_T in kcal/mole, k, in sec^{-1}.

[b] Data for benzene and naphthalene from reference 24. Data for acetone from Borkman, R.F., *Molec. Photochem., 4*, 453 (1972).

required for $S_1 \rightarrow T_1$ transitions and the greater probability of surface crossings between S_1 and T_1. For example, (Table 5.4) the lifetimes of naphthalene triplets increase from ~ 2 seconds to ~20 sec upon substitution of C-H for C-D and the lifetime of acetone triplets increase from 0.56 ms to 1.7 ms upon substitution of C-H for C-D.

The radiative lifetime of the triplet state of deuterated hydrocarbons nearly equals the maximum radiative lifetime - i.e., in the deuterated materials nearly every triplet emits whereas only a small fraction of the perprotio-aromatic triplets emit.[56] This striking result derives from Franck-Condon factors, in other words, f_ν is much smaller for C-D vibrations than for C-H vibrations. However, f_ν for C-D vibrations is ~20-30 times smaller than f_ν for C-H vibrations.[8b] For example, the triplet states of both perprotio- and perdeuterobenzene lie at 85 kcal/mole above S_0. This corresponds to about ten vibrational quanta for C-H vibrations. The lower amplitude of the C-D vibrations

requires a larger number of vibrational quanta to equal 85 kcal/mole. Therefore, the vibrational level of S_0 that is reached when the deuterated material converts from T_1 to S_0 possesses a large vibrational amplitude and intersystem crossing from T_1 to S_0 is inhibited. The same energy gap law for internal conversion (5.53) applies to T_1 to S_0 Intersystem crossing.

5.28 Perturbation of Spin-Forbidden Radiationless Transitions

The "heavy atom effect" is a term which has been coined to describe the influence of "heavy atom" substitution on spin-forbidden transitions.[19] For practical purposes, the atoms (e.g., C, N, O, F) in the first full row of the periodic table are considered “light” atoms. It is usually assumed that the dominant influence of the heavy atom effect measurably influences properties, let us assume that it influences all spin-forbidden transitions (radiationless, $S_1 \rightarrow T_1$, $T_1 \rightarrow S$, and radiative, $S_0 \rightarrow T_1$, $T_1 \rightarrow S_0$) but does not influence spin-allowed transitions (internal conversion, $S_1 \rightarrow S_0$ and fluorescence $S_1 \rightarrow S_0$). In this approximation the rate constants k_{ST}, k_{TS}, and k_P should be increased by the heavy atom effect but k_F and k_{IC} should not. In addition, the value of the extinction coefficient for singlet-triplet absorption, $\varepsilon(S_0 \rightarrow T_1)$should be enhanced by the heavy atom effect.

From Eqs. 5.31-5.37, we predict that the heavy atom effect will generally:

1. Decrease Φ_F (when k_{ST} is competitive with k_F for the "light atom" analogue)

2. Increase Φ_{ST} (when k_{ST} is competitive with k_F compared to the "light atom" analogue).

However, Φ_P and Φ_{TS} may either increase or decrease with heavy atom substitution depending on whether it is k_P or k_{TS} which is influenced to the greater extent.

From this analysis we deduce that heavy atom effects will not be universal. They will occur only when the heavy atom increases k_{ST} (k_P or k_{TS}) to a value which alters τ_S (or τ_T). Whether the heavy atom effect is manifested in a system depends of whether the additional spin-orbit coupling introduced by the heavy atom is comparable to the inherent spin-orbit coupling in a molecule and the rates of deactivation of the light atom analogue.

Empirically, the maximum heavy atom effect that is typically induced on k_{ST} by bromine atom substitution corresponds to a rate of the order of 10^8-10^9 sec^{-1}. As a result, if k_F or k_{ST} are of the order of 10^9 sec^{-1}or greater, a bromine atom may not produce a significant effect on the fluorescence lifetime or quantum yield. In practice, this means that heavy atom effects on $S_1 \rightarrow$ T intersystem crossing tend to be minimal for states which already possess substantial spin-orbit coupling (e.g., n,π* states) or very fast fluorescence rates (e.g., perylene).

5.29 Internal Perturbation of Intersystem Crossing

As an example of the heavy atom effect on k_{ST}^0, k_{TS}, and k_P^0 consider the data in Table 5.5. The heavy atom effect is most pronounced when the comparison light atom structure possesses inherently weak intersystem crossing and a slow rate of fluorescence deactivation. A classical exemplar is given by naphthalene and its halo derivatives. Both k_F^0 and k_{ST} are ~10^6 sec^{-1} for the light atom parent naphthalene. Substitution of F (considered a light atom) for H has, , as expected, relatively little effect on the emission efficiencies or rate constants of fluoro-naphthalene relative to naphthalene. However, substitution of Cl, then Br, then I leads to an ever-increasing decrease in Φ_F, and an accompanying increase in k_{ST} and k_P^0. The effect on Φ_P is not readily predictable (both k_P^0 and k_{TS} are influenced by the heavy atom).

As a second exemplar of the *lack of a heavy atom effect*, perylene[45] possesses a very fast and efficient fluorescence ($\Phi_F \sim 0.98$, $k_F^0 \sim 10^9$ sec^{-1}). If the heavy atom effect were the same for naphthalene and for perylene, then substitution of Br for H would increase k_{ST} to ~10^8 sec^{-1}. The lack of a heavy atom effect on k_F^0 when going from

perylene to bromoperylene can be understood in terms of a very fast inherent fluorescence which dominates the usual heavy enhancement of k_{ST}.

In going from anthracene to 9-bromoanthracene, a dramatic decrease in Φ_F and k_{ST} is noted. However, substitution of a second bromine atom (9-bromoanthracene→ 9,10-dibromoanthracene) results in an *increase* in Φ_F and decrease in k_{ST}. This "inverse" heavy atom effect is explained in terms of the influence of halogen substitution on the position of T_2. In anthracene k_{ST} occurs via a $S_1 \rightarrow T_1$ mechanism but in 9-bromoanthracene T_2 is lowered in energy so that it falls below S_1. Thus, a $S_1 \rightarrow T_2$ mechanism for intersystem crossing becomes available. Thus, $S_1 \rightarrow T_1$ or an activated $S_1 \rightarrow T_2$ intersystem crossing occurs. The net effect is to decrease k_{ST} relative to 9-bromoanthracene, although it is still large relative to anthracene. This exemplar indicates that a number of factors need to be considered when interpreting the overall effects of heavy atom substitution.

9,10-Dibromoanthracene offers an interesting example of how the energetic relationship of S_1 and T_n affects the value of k_{ST}.[46] In spite of the presence of two bromine atoms, 9,10-dibromoanthracene (DBA) still possesses a modest fluorescence yield ($\Phi_F \sim 0.05$). This implies that the "heavy atom" effect does not dominate and bring about very rapid intersystem crossing. Furthermore, the fluorescence yield of DBA is found to be extremely solvent-dependent. This peculiar behavior is understandable when it is realized that T_2 lies about 5 kcal/mole above S_1 for DBA. The energetic spacing of S_1 and T_2 requires that DNA either (a) undergoes activated intersystem crossing

---

Table 5.5 The Internal Heavy Atom Effect on Transitions between States[a]

Molecule	k_F^0	k_{ST}	k_P^0	k_{TS}	Φ_F	Φ_P
Naphthalene	10^6	10^6	10^{-1}	10^{-1}	0.55	0.05
1-Fluoronaphthalene	10^6	10^6	10^{-1}	10^{-1}	0.84	0.06
1-Chloronaphthalene	10^6	10^8	10	10	0.06	0.54
1-Bromonaphthalene	10^6	10^9	50	50	0.002	0.55

1-Endonaphthalene	10^6	10^{10}	500	100	0.000	0.70
Perylene		2×10^8 10^7	--	--	0.98	--
3-Bromoperylene		2×10^8 10^7	--	--	0.98	--

[a] Data for rigid solution at 77 K. At room temperature k_{TS} is often dominated by bimolecular deactivation of T_1 or by reactions of T_1. Rate constants are approximate.

from S_1 to T_2, or (b) undergoes direct intersystem crossing from S_1 to an upper vibrational level of T_1. Either mechanism will cause k_{ST} to be slowed down. The solvent effect is due to the shifting of the position of S_1 and T_2 as a function of solvent. In solvents such that $\Delta E(S_1 - T_2)$ is maximal, Φ_F is maximal.

5.30 External Perturbation of Intersystem Crossing

Examples of enhancement of the overall $S_1 \rightarrow T_1$ process by molecular oxygen (a paramagnetic species, containing no heavy atoms),[61] xenon,[62], organic halides,[63] and organometallics[64] are known. In the case of oxygen several mechanisms are possible, including enhancement of paramagnetic induced spin-orbit coupling and energy transfer (to produce a simultaneous $S_1 \rightarrow T_1$ transition in the perturbed molecule and a $T \rightarrow S$ transition in the oxygen molecule). The efficiency of the oxygen effect depends on the oxygen concentration and may be expressed as $k_{ST}^{O2}[O_2]$, where k_{ST}^{O2} is a bimolecular rate constant for oxygen perturbation and $[O_2]$ is the concentration of oxygen in the sample. The overall or observed rate of intersystem crossing (k_{ST}^{OB}) becomes

$$k_{ST}^{OB} = k_{ST} + k_{ST}^{O2}[O_2] \qquad (5.56)$$

Typical values of k_{ST}^{O2} are $\sim 10^{10} - 10^9$ M^{-1} sec^{-1}.[61] The solubility of O_2 in many organic solvents (under 1 atm of O_2) is $\sim 10^{-2}$M. Thus, $k_{ST}^{O2}[O_2] \sim 10^8$-$10^7$ sec^{-1}. Thus, the effect will be noticeable only if $k_{ST} \sim 10^8$ sec or less. For example, $\Phi_{ST} \sim 0.3$ for

pyrene ($k_{ST} \sim 10^7$ sec^{-1}) in the absence of O_2, and increases to ~1.0 under 1 atm of O_2. Similar effects are noted for xenon as a $S_1 \rightarrow$ T perturber.[62]

Although O_2 and Xe are known to be efficient quenchers of T_1 states, it is clear that not only enhancement of $T_1 \rightarrow S_0$ occurs, but other quenching pathways (including reaction) may occur. The role of molecular oxygen in molecular organic photochemistry will be examined in considerable detail in Chapter XX.

External heavy atom effects for heavy atoms that are not directly connect to aromatic cores are well established. As an illustration, consider the naphthalene derivatives **13** and **14**.[65]

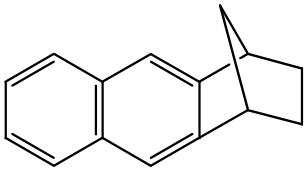

13

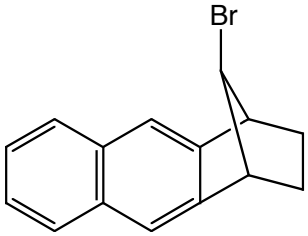

14

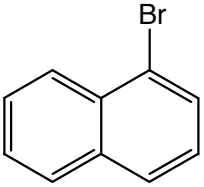

15

$k_{ST} = 2 \times 10^6$ sec^{-1} $k_{TS} = 2 \times 10^{-1}$ sec^{-1}

$k_{ST} = 300 \times 10^6$ sec^{-1} $k_{TS} = 40 \times 10^{-1}$ sec^{-1}

$k_{ST} = 500 \times 10^6$ sec^{-1} $k_{TS} = 600 \times 10^{-1}$ sec^{-1}

The effect of the "external" bromine in **14** is to enhance both k_{ST} and k_{TS}. The enhancement of k_{ST} is comparable to the "internal" effect of bromine on **15**. Note however, that k_{TS} is much higher for **15** than **14**. This may result from the somewhat different surface situation in **15** which may result in better Franck-Condon factors or better intersystem crossing.

5.31 The Relationship between Photophysical Radiationless Transitions and Photochemical Processes

In this chapter we have considered the photophysical radiationless pathways by which an electronically excited molecule can "find its way" back to its original ground state. If we view radiationless transitions in the general sense as a conversion of electronic energy into nuclear motion, then the distinction between "photophysical" and "photochemical" processes becomes blurred.[66] Indeed, we can imagine (Fig. 5.17) that they differ only in the degree of nuclear geometry change. If the distortion from an original ground state geometry is not too severe, return to the original geometry via radiationless transition(s) is possible. Suppose this transition takes place via the funnel on the excited surface shown in Figure 5.17. Relatively small changes in nuclear shape ("to the right" of the minimum) of the funnel will tend to deliver the molecule back to the ground state in a nuclear configuration that will favor formation of products rather than reactants. Thus, a photophysical transition which takes place through the funnel via transitions "to the left" of the minimum and returns the excited molecule to its original ground state may not differ qualitatively from photochemical transitions which produce products.

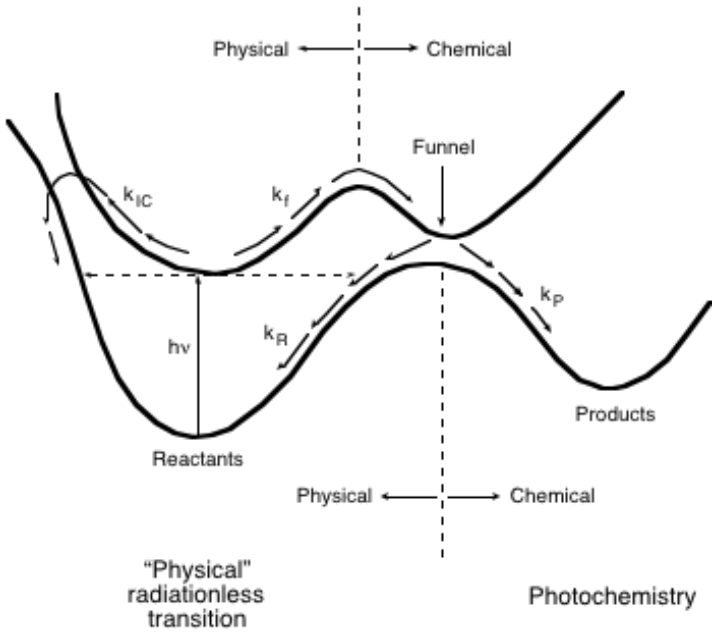

Figure 5.17 ***Schematic surface description of a possible relationship between "photophysical" and photochemical radiationless processes.***

In Chapters 4-14 we shall see that the notions of photophysical radiationless transitions and photochemical reactions are intimately related, via the common theory of energy surfaces.